Article

Immunity

Oncolytic Viruses Engineered to Enforce Leptin Expression Reprogram Tumor-Infiltrating T Cell Metabolism and Promote Tumor Clearance

Graphical Abstract

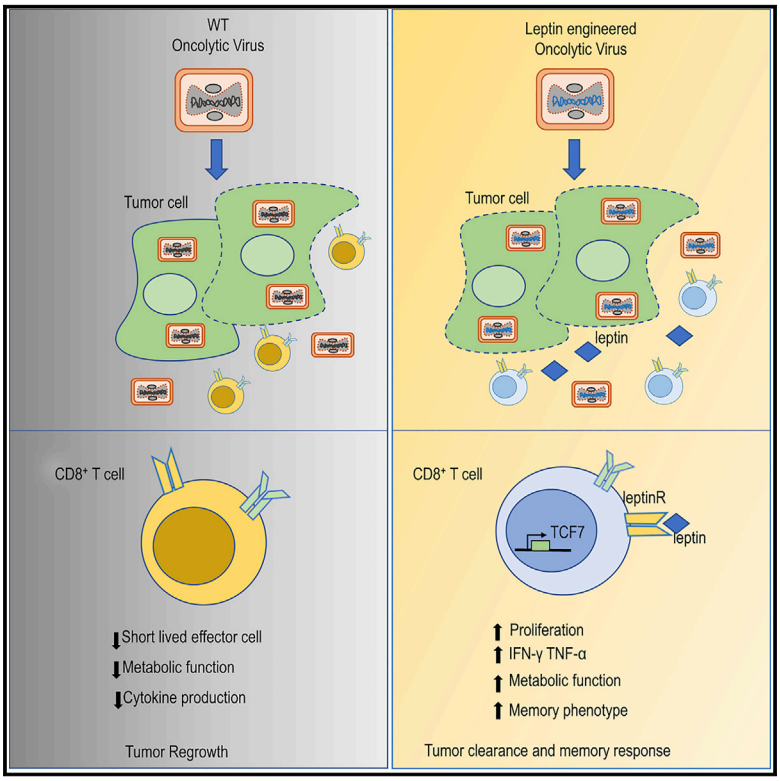

Highlights

- Single-cell sequencing reveals immune remodeling in *Vaccinia*-virus-treated tumors
- The adipokine leptin enhances T cell metabolic function *in vitro* and *in vivo*
- *Vaccinia* engineered to express leptin metabolically enhances antitumor responses
- Leptin-engineered *Vaccinia* promotes a memory response upon tumor rechallenge

Authors

Dayana B. Rivadeneira, Kristin DePeaux, Yiyang Wang, ..., Saumendra N. Sarkar, Stephen H. Thorne, Greg M. Delgoffe

Correspondence

delgoffeg@upmc.edu

In Brief

Metabolic insufficiency is a major barrier for antitumor immunity. Rivadeneira et al. demonstrate that engineering an oncolytic virus to express a metabolic modulator, in this case the adipokine leptin, improves T cell metabolic function in the tumor microenvironment, allowing a superior antitumor response compared to a control oncolytic.

Rivadeneira et al., 2019, Immunity *51*, 548–560
September 17, 2019
https://doi.org/10.1016/j.immuni.2019.07.003

CellPress

CellPress

Immunity
Article

Oncolytic Viruses Engineered to Enforce Leptin Expression Reprogram Tumor-Infiltrating T Cell Metabolism and Promote Tumor Clearance

Dayana B. Rivadeneira,[1,2] Kristin DePeaux,[1,2] Yiyang Wang,[1,2,5] Aditi Kulkarni,[4] Tracy Tabib,[3] Ashley V. Menk,[1,2] Padmavathi Sampath,[2] Robert Lafyatis,[3] Robert L. Ferris,[1,2,4] Saumendra N. Sarkar,[2] Stephen H. Thorne,[2] and Greg M. Delgoffe[1,2,4,6,*]

[1]Tumor Microenvironment Center, UPMC Hillman Cancer Center, Pittsburgh, PA, USA
[2]Department of Immunology, University of Pittsburgh, Pittsburgh, PA, USA
[3]Division of Rheumatology, University of Pittsburgh School of Medicine, Pittsburgh, PA, USA
[4]Head and Neck Cancer SPORE, University of Pittsburgh, Pittsburgh, PA, USA
[5]School of Medicine, Tsinghua University, Beijing, China
[6]Lead Contact
*Correspondence: delgoffeg@upmc.edu
https://doi.org/10.1016/j.immuni.2019.07.003

SUMMARY

Immunotherapy can reinvigorate dormant responses to cancer, but response rates remain low. Oncolytic viruses, which replicate in cancer cells, induce tumor lysis and immune priming, but their immune consequences are unclear. We profiled the infiltrate of aggressive melanomas induced by oncolytic *Vaccinia* virus using RNA sequencing and found substantial remodeling of the tumor microenvironment, dominated by effector T cell influx. However, responses to oncolytic viruses were incomplete due to metabolic insufficiencies induced by the tumor microenvironment. We identified the adipokine leptin as a potent metabolic reprogramming agent that supported antitumor responses. Leptin metabolically reprogrammed T cells *in vitro*, and melanoma cells expressing leptin were immunologically controlled in mice. Engineering oncolytic viruses to express leptin in tumor cells induced complete responses in tumor-bearing mice and supported memory development in the tumor infiltrate. Thus, leptin can provide metabolic support to tumor immunity, and oncolytic viruses represent a platform to deliver metabolic therapy.

INTRODUCTION

The successes associated with immunotherapy as a cancer treatment have resulted in a major shift in both cancer research and clinical practice, with a dominant focus on understanding and modulating immune activity at the tumor site. In solid tumors, immunotherapies using monoclonal antibody-mediated "checkpoint" blockade of Programmed Death 1 (PD-1) and cytotoxic T-lymphocyte-associated antigen 4 (CTLA-4) have resulted in durable responses, leading to US Food and Drug Administration (FDA) approval in a variety of indications (LaBeck et al., 2015; Mahoney et al., 2015). However, the reality of single-agent immunotherapies is that the majority of patients will not experience long-term durable benefits (Herbst et al., 2014; Weber et al., 2015). This resistance likely occurs for multiple reasons, but prominent among them are the failure to recruit T cells to the tumor and other, more dominant immunosuppressive mechanisms that limit T cell function in the tumor microenvironment (Sharma et al., 2017). Therefore, there is the need for new therapeutic modalities that could overcome these resistance mechanisms. Oncolytic virus immunotherapy is a class of therapeutic agent that has recently received more attention since the FDA approval in 2015 of a genetically modified herpes simplex virus, type 1 talimogene laherparepvec (T-VEC; Imlygic) (Andtbacka et al., 2015). Unlike checkpoint blockade approaches, oncolytic viruses have the ability to induce an immune response by triggering tumor-associated antigen and epitope spreading (Kanerva et al., 2013). Nonetheless, the approval of T-VEC was based on the durable remission rate of 16% in melanoma patients (Andtbacka et al., 2015), highlighting the ample space for improvement in this class of therapy, as well as further elucidation of its mechanisms of action. The exact cell populations involved in oncolytic virus-induced immune response is poorly understood, and the functional status of newly infiltrating lymphocytes has not been well studied.

It is now appreciated that the metabolism of both T cells and tumor cells represent key mechanisms limiting immune function against cancer. Cancer cells become metabolically deregulated, depleting the local environment of essential nutrients and producing an excess of potentially toxic by-products. In addition, tumor-infiltrating T cells acquire significant metabolic insufficiencies, including repressed glucose uptake and the loss of functional mitochondria. Thus, T cells are rendered insufficient in an environment that produces hypoxia and nutrient stress (Justus et al., 2015; Siska and Rathmell, 2015). Several groups including ours have demonstrated that metabolic reprogramming of T cells or modulation of the tumor microenvironment can result in increased antitumor immunity and response to immunotherapy (Rivadeneira and Delgoffe, 2018). Our group has shown that this metabolic reprogramming can be achieved by retroviral expression of metabolic genes in tumor-specific T cells, co-stimulation via the 41BB receptor, and pharmacologic

remodeling of the tumor microenvironment using the type 2 diabetes drug metformin (Menk et al., 2018; Scharping et al., 2016, 2017). However, the use of genetically encoded, protein-based soluble factors such as adipokines for immunometabolic modulation remains unstudied.

Leptin is a canonical adipokine with potent metabolic reprogramming functions (Pérez-Pérez et al., 2017) such as the promotion of glucose and fatty oxidation and mitochondrial biogenesis (Saucillo et al., 2014; Steinberg et al., 2002). While discovered and typically studied in the context of obesity, T cells express the leptin receptor, and leptin levels have been associated with inflammatory states (Abella et al., 2017). T cells stimulated in the context of leptin can synthesize more cytokines and increase their proliferation (Dixit et al., 2004; Howard et al., 1999; Lord et al., 1998). Nonetheless, to date, the study of leptin in immunity has been largely assessed in the context of obesity and not ascertained therapeutically.

In this study, we used single-cell RNA sequencing to deeply profile the infiltrate of aggressive melanomas induced by oncolytic *Vaccinia* virus, revealing that oncolytic viruses promote the infiltration of a robust tumor infiltrate, but one that is ultimately ineffective at promoting complete responses, due in part to metabolic insufficiency. We next explored the utility of leptin as a tool to overcome the observed metabolic insufficiency by promoting the metabolic reprogramming of tumor-infiltrating T cells. Using a melanoma model in which leptin is locally elevated in the tumor microenvironment, we showed potent T cell activation and tumor control that was linked to metabolic reprogramming. Thus, we engineered oncolytic *Vaccinia* virus to genetically express leptin in order to deliver it to the tumor microenvironment. This therapy resulted in complete therapeutic responses, compared to the partial responses obtained with wild-type oncolytic virus. Leptin expressing *Vaccinia* virus simultaneously lysed tumor cells, leading to the stimulation of new T cell infiltration, while also metabolically supporting the activity of that infiltrate through the local secretion of leptin.

RESULTS

Oncolytic *Vaccinia* Virus Treatment of Tumors Resulted in the Remodeling of the Tumor Immune Microenvironment

While the oncolytic virus T-VEC is an FDA-approved immunotherapy for cancer treatment, the immune consequences of this agent are unclear. We sought to systematically profile the immune infiltrate induced by oncolytic virus infection. One major limitation of oncolytic virus therapy is that many viruses, including T-VEC, do not replicate efficiently in hypoxia (Friedman et al., 2012; Pipiya et al., 2005). Thus, we used oncolytic *Vaccinia* virus, which is easily engineered, encodes its own polymerase, and maintains replicative function in hypoxic tumor cells (Hiley et al., 2010; Moss, 2013). We used the Western Reserve laboratory strain *Vaccinia* virus, which harbors a genetic deletion of thymidine kinase, and *Vaccinia* growth factor genes that generate a potent oncolytic viral agent (Buller et al., 1985; Puhlmann et al., 2000; Whitman et al., 1994). We used a melanoma cell line called clone 24 (CL24), generated in our lab from a single cell of a $Pten^{f/f}Braf^{LSL.V600E}Tyr2^{Cre.ER}$ mouse that developed melanoma after tamoxifen administration (Dankort et al., 2009; Najjar et al., 2019). This cell line is syngeneic to C57/BL6 mice and carries driver mutations that are common in human melanoma (as opposed to the often-used B16). CL24 is poorly infiltrated and is completely insensitive to monoclonal antibody against PD1 (anti-PD1 monotherapy) (Najjar et al., 2019). A single dose of *Vaccinia* virus was injected intratumorally when tumors reached 4 mm, which resulted in substantial tumor regression but no complete responses (Figure 1A). We thus sought to determine the character of the tumor infiltrate induced by oncolytic viruses by using single-cell RNA sequencing of the $CD45^+$ tumor-infiltrating leukocytes of PBS-treated or *Vaccinia*-infected CL24 tumors. We first used unsupervised clustering data analysis to separate the $CD45^+$ cells into distinct groups of immune populations (Figure 1B). These immune populations were then classified based on the expression of the known markers for each population (Figures S1A and S1B). These analyses were conducted prior to regression. Our data identified known immune cell populations when analyzed in aggregate; however, analysis based on treatment group revealed that oncolytic *Vaccinia* virus immunotherapy induced changes in the tumor immune microenvironment (Figure 1C). Our data revealed that *Vaccinia*-infected tumors showed an influx of new, effector-like $CD8^+$ T cells, natural killer (NK) cells and monocytes, and a proportional loss of dysfunctional or suppressive cells like myeloid-derived suppressor cells (MDSCs) and tumor-associated macrophages compared to PBS-treated tumors (Figure 1C). RNA sequencing analysis showed that oncolytic *Vaccinia* virus induced a remodeling of the tumor immune microenvironment, but one that ultimately succumbs to tumor-induced immunosuppression and eventual outgrowth.

Oncolytic *Vaccinia* Virus Promoted Non-exhausted T Cell Infiltration with Severe Metabolic Deficiencies

Flow cytometric analysis of the tumor-infiltrating lymphocytes from oncolytic virus-treated mice confirmed that the influx of new immune cells appeared to be dominated by $CD8^+$ T cells, while we observe a decreased representation of regulatory T cells in the $CD4^+$ compartment (Figure 2A). Analysis of the co-inhibitory marker expression showed that these "new" $CD8^+$ T cells have protein expression of T cell immunoglobulin and mucin containing 3 (Tim-3) alone (Figure 2B), as well as a low to mid-expression of PD1 (Figure 2C), suggesting that these cells are not reinvigorated tumor residents but rather new immigrants that are not yet fully exhausted T cells. While co-inhibitory molecule expression is associated with T cell dysfunction, we and others have also shown that metabolic insufficiency can predict T cell function (Scharping et al., 2016). We further analyzed mitochondrial content as a marker for metabolic sufficiency, revealing that despite the "non-exhausted" co-inhibitory molecule pattern of expression, tumor-infiltrating lymphocytes from oncolytic virus-treated tumors were still metabolically insufficient, as is evident by the lack of change in MitoTracker staining compared to untreated tumors (Figure 2D). Overall, *Vaccinia* virus-induced oncolysis reprograms the immune microenvironment, promoting an influx of new T cells that ultimately succumb to metabolic insufficiency.

Leptin Metabolically Reprogrammed Activated T Cells

Given that oncolytic viruses stimulated new immune infiltrates that still succumbed to metabolic dysfunction, we next sought to explore ways to bolster those new T cells such that they would

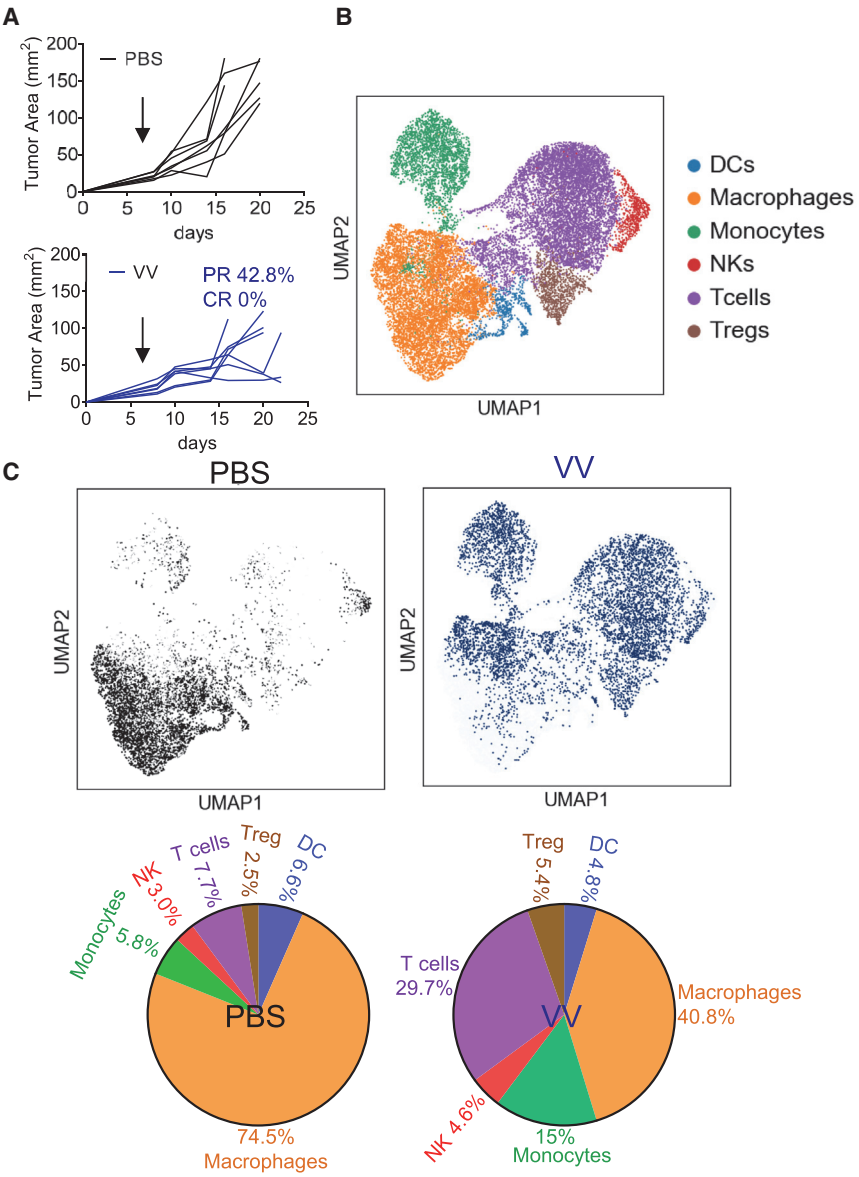

Figure 1. Oncolytic *Vaccinia* Virus Has Potent Immunostimulatory Activity

(A) C57BL/6J mice were injected subdermally with CL24 cells. Tumors were treated intratumorally with PBS and control *Vaccinia* virus (VV) at 2.5×10^6 PFU, and tumor growth was monitored. Each line represents an individual mouse.

(B) Single-cell RNA-seq data for 4,000 $CD45^+$ sorted cells treated as in (A). Cells were extracted on day 7. Data were generated by unsupervised clustering through Seurat.

(C) Uniform Manifold Approximation and Projection (UMAP) analysis and quantification of PBS- and VV-treated mice. Population percentages were determined out of the percentage of all $CD45^+$ cells. Data represent n = 2 per condition. See also Figure S1.

be more competitive in the tumor microenvironment. We also wished to use a genetically encoded payload, so that this agent could be encoded in the viral vector. As previously discussed, leptin is a cytokine that modulates energy homeostasis and promotes an inflammatory response (La Cava and Matarese, 2004). We first sought to determine the metabolic reprogramming functions of leptin on T cells. We activated $CD8^+$ T cells isolated from peripheral lymph nodes (LNs) and cultured cells in increasing concentrations of leptin. Leptin induced increases in both the basal oxygen consumption rate and the spare respiratory capacity (a measure of mitochondrial reserve that defines long-lived memory T cells; Dixit et al., 2004) of $CD8^+$ T cells (Figure 3A), but they had little effect on the ability of activated T cells to perform glycolysis as measured by extracellular acidification (Figure 3B). Flow cytometry analysis reinforced these data, showing an increase in mitochondrial mass under leptin exposure that was indicative of higher oxidative phosphorylation, while observing no changes in glucose uptake (Figure 3C). The short-term treatment of activated T cells with leptin revealed the increased activation of phospho-p38 mitogen-activated protein kinase (MAPK) and the consequent activation of the transcription factor ATF-2, which we and others have previously shown to be critical for mitochondrial biogenesis (Akimoto et al., 2005; Menk et al., 2018) (Figure 3D). Thus, leptin can stimulate T cells to increase their oxidative activity and capacity, a metabolic reprogramming event that is highly desirable in the tumor microenvironment.

We assessed the expression of the leptin receptor in murine T cells, confirming the expression of the leptin receptor in T cells, as previously observed (Lord et al., 1998) (Figure 3E). Furthermore, melanoma tumor-infiltrating lymphocytes expressed more leptin receptor compared to T cells in the LNs (Figure 3E). Categorizing the tumor-infiltrating lymphocytes according to the expression of the co-inhibitory molecules, we observed a higher expression of the leptin receptor in activated or exhausted T cells with a high expression of PD1 and Tim-3 (Figure 3F). Thus, leptin can promote metabolic reprogramming in T cells, and tumor-infiltrating T cells bear its receptor.

Elevating Local Leptin Protein Concentrations in the Tumor Microenvironment Enabled Antitumor Immunity

The therapeutic effects of leptin in the context of tumor-infiltrating lymphocytes have not been previously investigated. We hypothesized that leptin can enhance the metabolic capacity of tumor-infiltrating lymphocytes, consequently enhancing their function in the tumor. The initial studies treating tumor-bearing mice with recombinant leptin showed that systemic delivery, even at relatively high doses, did not have any effects on tumor growth or tumor-infiltrating lymphocyte makeup (Figure S2A). The intratumoral administration of leptin showed small

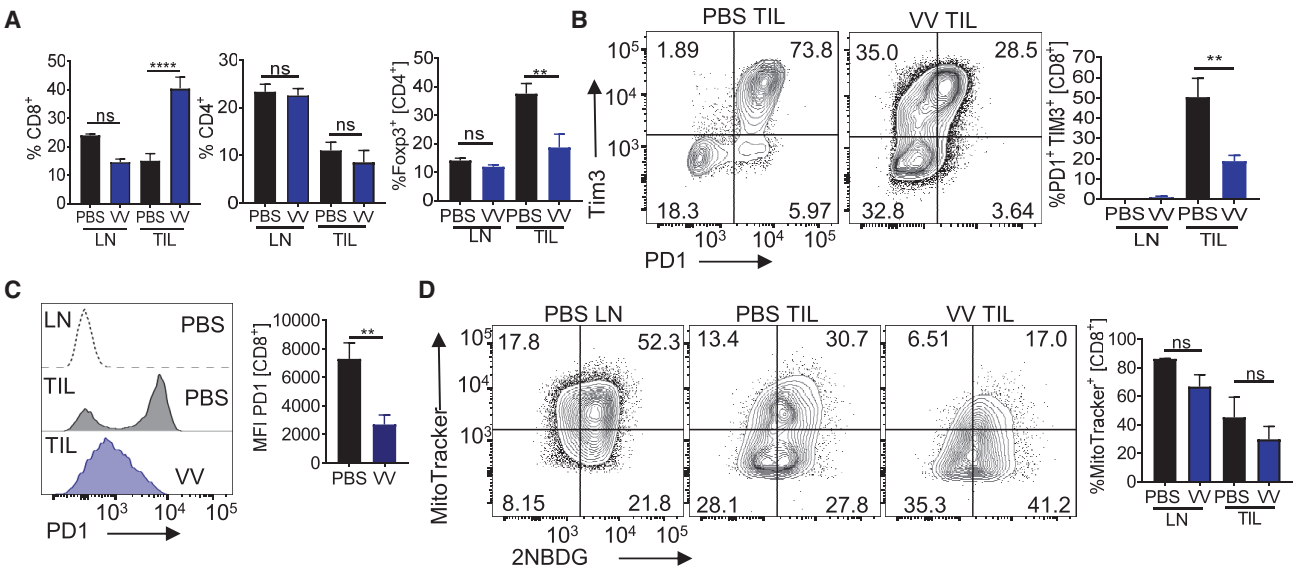

Figure 2. Tumor-Infiltrating Lymphocyte Analysis of Oncolytic *Vaccinia*-Virus-Treated Tumors Shows Non-exhausted T Cell Infiltration with Metabolic Deficiencies

(A) C57BL/6J mice were injected subdermally with CL24 cells. Tumors were treated intratumorally with PBS and control *Vaccinia* virus (VV) 5–7 days after tumor cell injection. CD8, CD4, and Foxp3 expression analysis on LNs and tumor-infiltrating lymphocytes (TILs) is shown, as are tabulated flow cytometric data.

(B) Expression of inhibitory molecules PD1 and Tim-3 from mice treated as in (A). Representative flow cytogram of PD1 and Tim-3 staining in LNs and TILs and tabulated flow cytometric data are shown.

(C) Representative histogram PD1 expression on $CD8^+$ T cells and tabulated data.

(D) Mitochondrial content analyzed by MitoTracker staining in $CD8^+$ T cells from mice treated as in (A). Representative flow cytogram of MitoTracker against 2-NBD-glucose (2NBDG) staining in LNs and TILs and tabulated flow cytometric data are shown. Data represent at least three independent experiments.

*p < 0.05, **p < 0.01, and ***p < 0.001 by paired t test. ns, non-significant. Error bars indicate SEMs.

but not significant changes, suggesting that leptin may need to be more effectively delivered locally to bolster intratumoral immunity (Figure S2A). To test the metabolic reprogramming functions of leptin in isolation (outside oncolytic virus infection), we instead engineered CL24 cells to express an empty vector ($CL24^{hygro}$) or leptin ($CL24^{leptin}$). $CL24^{leptin}$ cells expressed leptin intracellularly (Figure S2B) and released it into culture supernatant (Figure S2C). *In vitro*, $CL24^{leptin}$ showed comparable growth kinetics with CL24 expressing a control plasmid ($CL24^{hygro}$) (Figure S2D). However, when $CL24^{leptin}$ cells were injected subdermally into C57BL/6J mice, they grew at a substantially slower rate compared to $CL24^{hygro}$ controls (Figure 4A) and have significantly prolonged survival (Figure 4B), suggesting that leptin may stimulate host immunity. The depletion of $CD8^+$ T cells (Figure S2E) revealed that the controlled tumor growth observed in $CL24^{leptin}$ tumors required functional immunity (Figure 4C). To determine whether this increased antitumor immunity was due to leptin acting on T cells, we injected control or leptin-overexpressing CL24 into mice bearing a T cell-restricted heterozygous deletion of the leptin receptor. The leptin receptor is haploinsufficient (Coleman, 1979), and T cells from these mice have a lower protein expression of the leptin receptor (Figure S2F). In these mice, leptin-overexpressing tumors were not controlled by the immune system, mirroring total CD8 T cell depletion (Figure 4D). Thus, locally elevating leptin in the tumor microenvironment acted directly on T cells to induce immune-mediated tumor growth control. Analysis of the tumor-infiltrating lymphocytes at day 10 (when tumors were of a comparable size between groups) showed an increased percentage of $CD8^+$ T cells in tumors overexpressing leptin compared to control tumors (Figure 4E). CL24 expresses gp100, so we directly tested the ability of the leptin-overexpressing tumor to be infiltrated using an adoptive transfer of activated Pmel $CD8^+$ T cells. These data show a significant increase in infiltration 72 h post-adoptive transfer (Figure S3A). We also noted that leptin-overexpressing CL24 tumors had increased numbers of NK cells, but not other immune populations such as B cells (Figure S3B). Thus, the engineered overexpression of leptin in melanoma cells resulted in a tumor infiltrate that is more biased toward type 1 immunity, and localized expression of leptin controls tumor growth by enhancing a $CD8^+$ T cell-dependent antitumor response.

Leptin Metabolically Improved the Function of Tumor-Infiltrating Lymphocytes

We next wanted to determine whether leptin merely promoted the increased infiltration of T cells or whether T cells were functionally improved. $CD8^+$ T cells infiltrating leptin-overexpressing tumors synthesized the elevated protein expression of interferon-γ (IFN-γ) and tumor necrosis factor α (TNF-α) upon re-stimulation with phorbol 12-myristate 13-acetate (PMA) and ionomycin (Figures 4F and S2G). In addition, $CD8^+$ T cells that infiltrated leptin-expressing tumors were more proliferative *in situ* as measured by Ki67 staining (Figures 4G and S2H). Consistent with our *in vitro* signaling analyses and prior work in other systems (Sanchez-Margalet and Martin-Romero, 2001), T cells

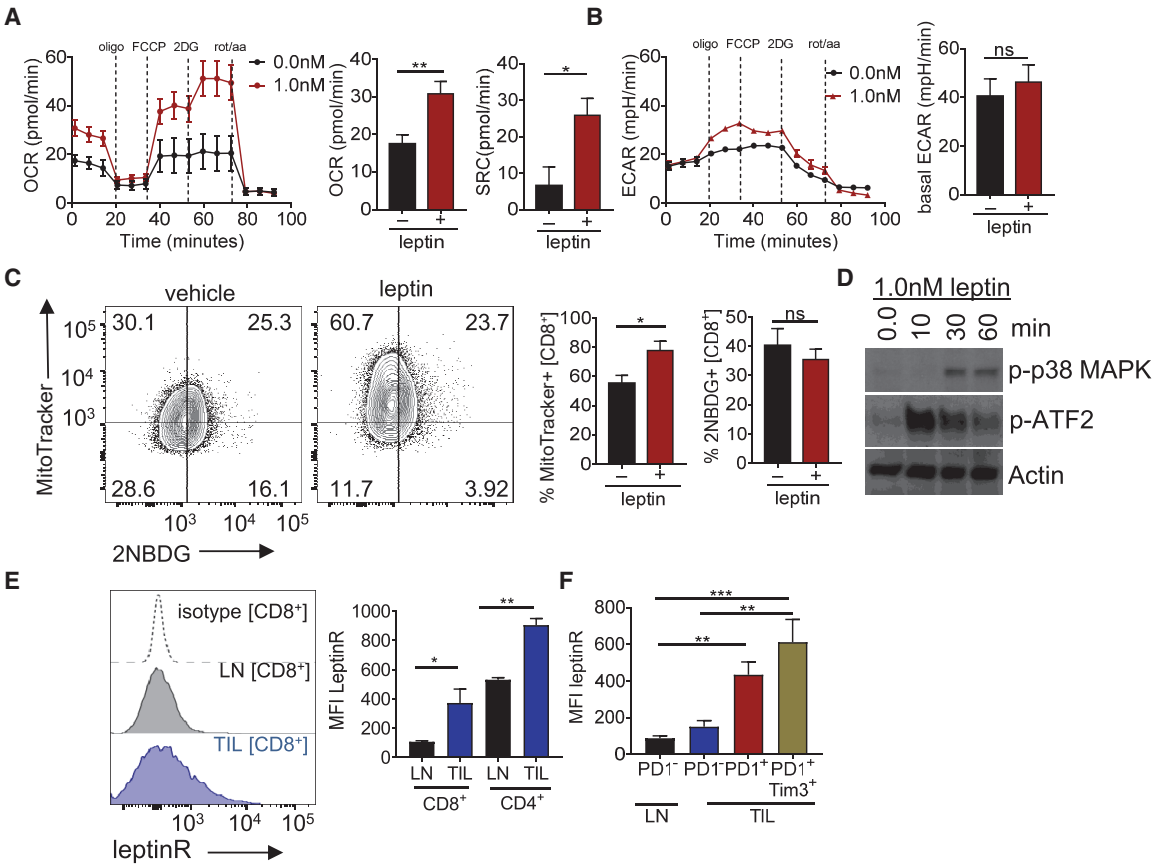

Figure 3. The Leptin Receptor Is Upregulated in Tumor-Infiltrating T Cells, and Leptin Is Capable of Metabolic Reprogramming

(A) Representative oxygen consumption rate (OCR) trace and tabulated OCR and spare respiratory capacity (SRC) of $CD8^+$ T cells activated with 3 μg/mL immobilized anti-CD3 in the presence of anti-CD28 (2 μg/mL) for 24 h. Cells were treated with 0.0, 0.1, and 1.0 nM mouse recombinant leptin for 24 h.

(B) Representative extracellular acidification rate (ECAR) trace for cells treated as (A).

(C) Mitochondrial content analyzed by MitoTracker staining and glucose uptake by 2NBDG staining in $CD8^+$ T cells from mice treated as in (A). Representative flow cytogram of MitoTracker against 2NBDG staining in LNs and tumor-infiltrating lymphocytes (TILs) and tabulated flow cytometric data.

(D) T cells day 5 after activation treated with 1.0 nM recombinant leptin and harvested at 10, 30, and 60 min. Immunoblot of p-p38MAPK and phospho-activating transcription factor 2 (p-ATF2); actin was used as a loading control.

(E) Leptin receptor staining of $CD8^+$ T cells from mouse LNs and TILs from tumor-bearing mice.

(F) Leptin receptor expression staining of PD1 and Tim-3 in $CD8^+$ T cells in LNs and TILs. Data represent at least three independent experiments. *$p < 0.05$ by unpaired t test. Error bars indicate SEMs.

Data represent at least three independent experiments. *$p < 0.05$, **$p < 0.01$, and ***$p < 0.001$ by paired t test. Error bars indicate SEMs.

infiltrating leptin-overexpressing tumors had a higher steady-state phosphorylation of AKT, signal transducer and activator of transcription 3 (STAT3), and p38-MAPK (Figure S3C). T cells from leptin-overexpressing tumors, consistent with our metabolic analyses *in vitro*, had increased mitochondrial mass, suggesting that leptin was acting on the T cells to mediate metabolic reprogramming (Figure 4H). Glucose uptake was unchanged in the tumor-infiltrating lymphocytes of $CL24^{leptin}$ (Figure 4H), although this may be due to other inhibitory mechanisms in the tumor microenvironment (Chang et al., 2015; Ho et al., 2015). However, co-inhibitory receptor expression was unchanged in these cells (Figure S3D). This is consistent with our previous studies using various types of metabolic reprogramming (Scharping et al., 2016, 2017). Thus, while these cells may appear more phenotypically "exhausted" (Figure S3D), with a similar high $PD1^+$ $Tim\text{-}3^+$ expression in both groups, leptin-induced metabolic support allowed cells to mediate tumor control and be polyfunctional and proliferative.

Leptin Expressing Oncolytic *Vaccinia* Virus Induced Superior Antitumor Responses

We next sought to locally elevate leptin through delivery by oncolytic virus. To generate a leptin expressing *Vaccinia* virus, the leptin gene (*Lep*) was cloned in the luciferase expressing the pSC65 vector under the control of the *Vaccinia* p7.5 promoter. Leptin containing recombinant *Vaccinia* virus (VV^{leptin}) and control luciferase expressing virus (VV) were generated and used to infect CL24 cells. We analyzed the expression of leptin in CL24 cells 24 and 48 h post-infection (Figure S4A), as well as the release of leptin in the media (Figure S4B). Mice harboring CL24 tumors were treated with VV or VV^{leptin} with a dose of 2.5×10^6 plaque-forming units (PFUs) intratumorally, which

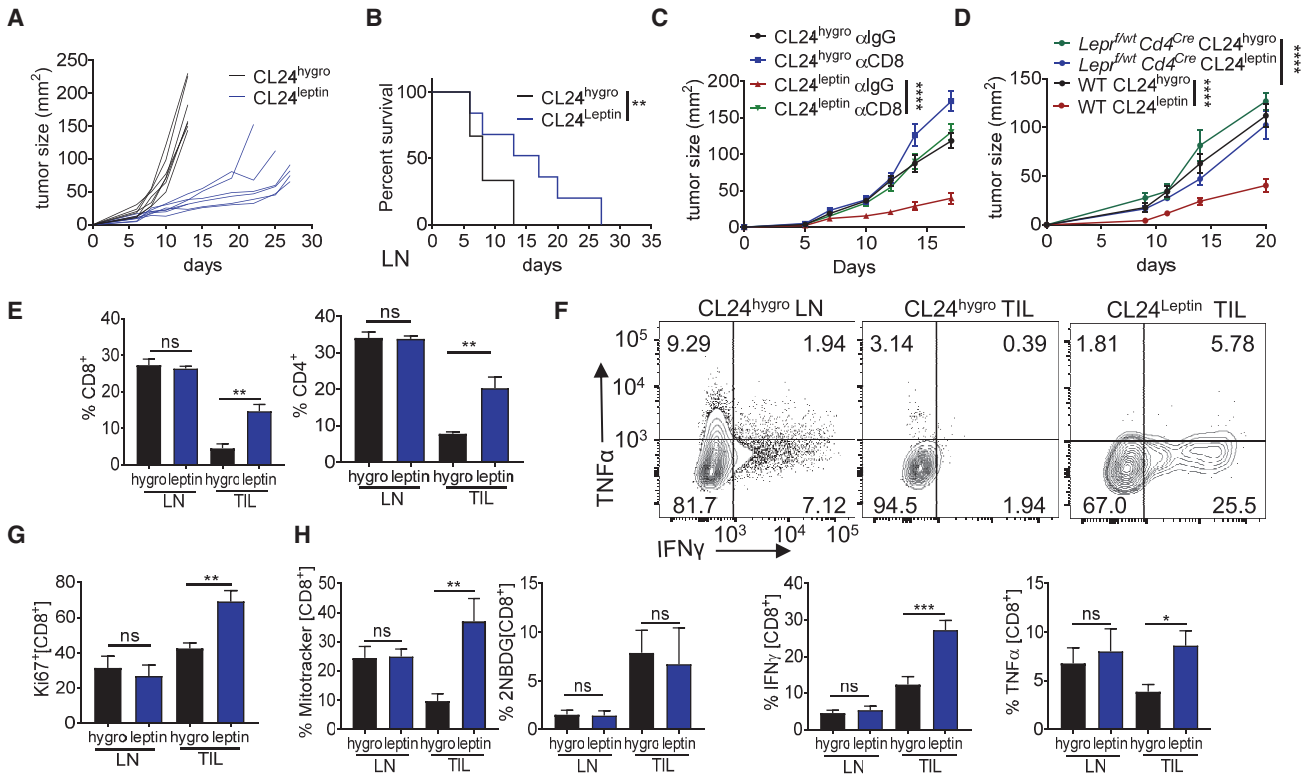

Figure 4. Expression of Leptin in Cancer Cells Results in Immune-Mediated Tumor Control and Metabolically Improves the Function of Tumor-Infiltrating Lymphocytes

(A) CL24^{hygro} and CL24^{leptin} were injected subdermally in C57BL/6J mice, and tumor growth was monitored. Each line represents an individual mouse.

(B) Survival plot of mice treated as in (A).

(C) C57BL/6J mice were treated every other day with anti-CD8 (200 μg). At day 6, the mice were injected with either CL24^{hygro} or CL24^{leptin}, and tumor growth was monitored.

(D) Leptin receptor flox CD4^{cre} heterozygous mice (Lepr$^{f/wt}$ CD4^{cre}) and wild-type mice were injected with either CL24^{hygro} or CL24^{leptin}, and tumor growth was monitored.

(E) CD8 and CD4 expression analysis on LNs and tumor-infiltrating lymphocytes (TILs) from mice injected with CL24^{hygro} and CL24^{leptin}.

(F) Representative flow cytograms of LNs and TILs from mice injected with CL24^{hygro} and CL24^{leptin}. Cells were stimulated overnight with PMA and ionomycin for cytokine production analysis by staining for IFN-γ and TNF-α of CD8$^+$ T cells. Tabulated flow cytometric data are shown.

(G and H) Tabulated flow cytometric data for CD8$^+$ T cells from LNs and TILs from mice injected with CL24^{hygro} and CL24^{leptin} analyzed for Ki67 expression (G) and metabolic markers MitoTracker FM staining and 2NBDG uptake (H).

Data represent at least three independent experiments. *p < 0.05, **p < 0.01, and ***p < 0.001 by paired t test. Error bars indicate SEMs. See also Figures S2 and S3.

was sufficient to induce luciferase expression specifically in the tumor (Figure S4D) and detect free leptin in the tumor interstitial fluid; white adipose (WA) tissue interstitial fluid acted as a positive control (Figure S4C). Leptin-engineered virus still retained oncolytic activity *in vitro*, inducing substantial cell death of CL24 cells after infection (Figure S4E).

We treated CL24-melanoma-bearing mice after an established tumor was formed, when these tumors could be reliably intratumorally injected (4 mm in one direction). Notably, in all of our studies, mice received a single therapeutic dose of oncolytic virus. Consistent with our previous results, all of the mice injected with the control virus experienced partial responses, leading to eventual tumor outgrowth. The partial response to the control virus was especially exciting, as this aggressive melanoma line is completely resistant to anti-PD1 immunotherapy (Najjar et al., 2019). In contrast to mice treated with VV, those injected with the same dose of VV^{leptin} had larger regressions, including a substantial proportion of complete responses (27%) (Figure 5A). This resulted in a significant survival advantage for these mice (Figure 5B). We observed no changes in body weight between all three treatments (Figure S4F). More immunogenic tumor models, such as the anti-PD1-sensitive model MC38, received no added benefit from leptin-engineered virus (Figure S4G), suggesting that leptin-mediated metabolic support may be especially important in immunologically harsh environments. Thus, we also used the aggressive pancreatic tumor model Panc02, which is characterized by a very poor therapeutic response to contemporary therapies. A single intratumoral dose of VV^{leptin} mediated a substantially improved response and survival compared to VV, which afforded essentially no measurable benefit (Figures 5C and 5D).

Work from other groups suggests that obesity may be associated with better responses to anti-PD1-based immunotherapy (Wang et al., 2019). Anti-PD1 likely functions through mechanisms

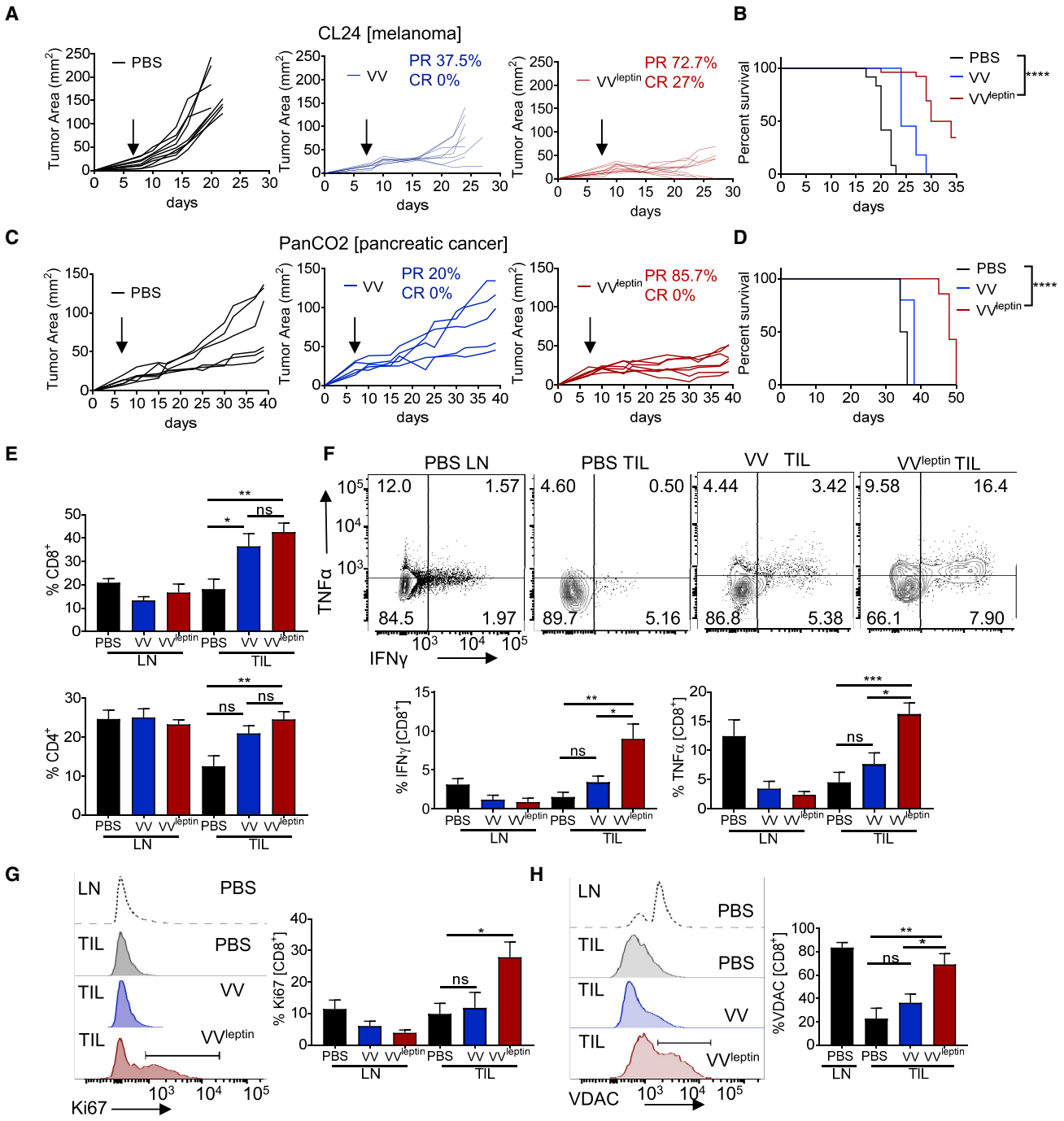

Figure 5. Leptin-Engineered *Vaccinia* Virus Promotes Improved Antitumor Immune Response through Metabolic Reprogramming

(A) C57BL/6J mice were injected subdermally with CL24 cells. Tumors were treated intratumorally with PBS (n = 8), VV (n = 8), or VV^{leptin} (n = 10) at 2.5 × 10^6 PFU, and tumor growth was monitored. Each line represents an individual mouse.

(B) Mice were monitored for survival as in (A).

(C) C57BL/6J mice were injected subdermally with Panc02 cells. Tumors were treated as in (A) 7–10 days after tumor cell injection.

(D) Mice were monitored for survival as in (C).

(E) On day 10 after treatment, lymphocytes were isolated from tumor-infiltrating lymphocytes (TILs) and LNs. Tabulated flow cytometric data for CD8 and CD4 expression are shown.

(F) Isolated lymphocytes were stimulated overnight with PMA and ionomycin. Tabulated flow cytometric data for cytokine production analysis by staining for IFN-γ and TNF-α are shown.

(legend continued on next page)

that are distinct from oncolytic viruses, but nevertheless we sought to determine how obesity (in which leptin is systemically elevated) may affect VV therapy, with or without our engineered construct. Mice treated with VV had the same tumor growth kinetics when comparing lean mice with obese mice. Leptin-engineered virus provided no additional benefit to obese mice (Figure S4H), which we hypothesize may be due to the fact that obese mice are rendered insensitive to leptin (Wang et al., 2019). Furthermore, anti-PD1 does not provide further therapeutic benefit to VV^{leptin} in lean mice (Figure S4I). The greatest therapeutic benefit was observed when lean mice were treated with VV^{leptin}, inducing complete responses in anti-PD1-insensitive tumor models.

Leptin-Engineered *Vaccinia* Virus Therapy Promotes a Memory Response to Secondary Tumor Challenge

Consistent with our prior single-cell RNA sequencing (scRNA-seq) data, analysis of immune infiltrate in tumors treated with VV and VV^{leptin} showed that both oncolytic viruses induced an increase in T cell infiltration at the tumor site (Figure 5E). Furthermore, analysis of $CD8^+$ T cells infiltrating treated tumors revealed that VV^{leptin} induced a qualitatively superior tumor infiltrate: increased T cell activity at the tumor site shown by an increase in cytokine competency (Figure 5F) and increased proliferative capacity (Figure 5G). Furthermore, we observed no difference in the expression of PD1 and Tim-3 between VV and VV^{leptin} treatments (Figure S4J). Consistent with our data in T cells infiltrating leptin-overexpressing tumors, $CD8^+$ T cells in tumors treated with VV^{leptin} exhibited an increase in mitochondrial mass as measured by the mitochondrial protein VDAC (Figure 5H) and MitoTracker staining (Figure S5A), suggesting that T cells infiltrating this leptin-reprogrammed microenvironment are more metabolically sufficient.

We conducted an unsupervised clustering of T lymphocytes from scRNA-seq in control, VV, and VV^{leptin} tumors defining T cell populations (Figure 6A). Unsupervised clustering confirmed our flow cytometric findings: T cells in tumors responding to leptin-engineered virus treatment were not in greater numbers (compared to control virus treatment), but their phenotype was changed (Figure 6B). Notably, we saw increases in effector memory and memory signature (Figure 6B). We also saw changes in the macrophage compartment, suggesting a potential switch to a more inflammatory state (Figures S6A and S6B). Leptin has been shown to inhibit regulatory T cells (T_{reg}) and modulate the inflammatory response in autoimmune diseases (De Rosa et al., 2007; Klingenberg et al., 2010; Matarese et al., 2001). Furthermore, previous work has shown that oncolytic virus therapy can reduce the infiltration of T_{reg} cells (Barve et al., 2008; Ricca et al., 2018). Consistently, after oncolytic virus treatment of VV and VV^{leptin}, we observed a decrease in the percentage of the T_{reg} population compared to PBS treatment with a comparable percentage of the population between VV and VV^{leptin} (Figure S5D), suggesting that leptin was not necessarily acting at the level of T_{reg} cell modulation.

As oncolytic viruses have been purported to induce new T cell priming to viral and tumor antigens (Brown et al., 2017; Russell and Barber, 2018), we next wanted to ascertain the effects of our treatments on the T cell repertoire at the tumor site. T cell receptor (TCR) sequencing revealed that while PBS-treated tumors had few infiltrating T cells dominated by an oligoclonal population, treatment with *Vaccinia* resulted in a substantial influx of new T cells with a polyclonal repertoire (Figure 6C). Leptin-engineered *Vaccinia* had a slightly less clonal population, suggesting that at this time point (7 days after viral treatment) some clones were preferentially expanding (Figure 6D). Tyrosinase-related protein 2 (TRP2) tetramer-binding cells were similar or underrepresented in the virus-treated tumors (Figure S5B), suggesting that the majority of this tumor infiltrate was specific to previously hidden antigens that were revealed by oncolysis. The clonal expansion could be indicative of the expansion of some memory precursors, and leptin-engineered VV induced a greater percentage of $CD127^{hi}$ memory precursors (Figure 6E). Furthermore, while we observed a trend (but not statistically significant) toward an increase in $KLRG1^{hi}CD127^+$ memory precursors (Figure 6F), TCF7, a transcription factor responsible for the formation of the memory response of central CD8 T cells (Zhou et al., 2010), was upregulated even in $KLRG1^+$ effector T cells (Figure 6G).

A concern with oncolytic viruses is that the immunity they may elicit may be dominated by virus-specific cells. An elevated percentage of *Vaccinia*-derived B8R tetramer binding cells was evident in the infiltrate of leptin and control virus-infected tumors (Figure S5C). However, when the survivors of VV^{leptin}-treated tumor-bearing mice were rechallenged with uninfected, wild-type CL24 cells after complete responses, most of the mice completely rejected their tumors, while the minority that grew out were substantially slower compared to naive mice (Figure 6H). Thus, while antiviral immunity is certainly primed in oncolytic VV-treated mice, the leptin-engineered virus was able to promote a strong memory response to subsequent tumor challenge. As memory T cells have increased mitochondrial reserve and depend on that reserve for their memory function (van der Windt et al., 2013), leptin may preferentially support the memory phenotype in the face of inflammation and oncolysis in the tumor microenvironment. Our data suggest that by providing metabolic support to newly infiltrated T cells induced by oncolytic virus treatment, memory precursor populations with superior antitumor capabilities can preferentially expand and mediate complete responses.

DISCUSSION

Among the many challenges encountered by the immune response in solid tumors is the poor capacity to infiltrate and being able to carry out their effector function appropriately in a hostile microenvironment. Our study shows that we can overcome both obstacles by engineering an oncolytic virus that can deliver metabolic modulation (in the form of the adipokine leptin) directly

(G) Tabulated flow cytometric data for $CD8^+$ T cells from LNs and TILs from mice treated as in (A) were analyzed for Ki67 expression.

(H) Representative histograms and tabulated flow cytometric data of $CD8^+$ T cells isolated from LNs and TILs were analyzed for mitochondrial protein VDAC.

Data represent at least three independent experiments. *$p < 0.05$, **$p < 0.01$, and ***$p < 0.001$ by two-way ANOVA. Error bars indicate SEMs. See also Figures S4 and S5.

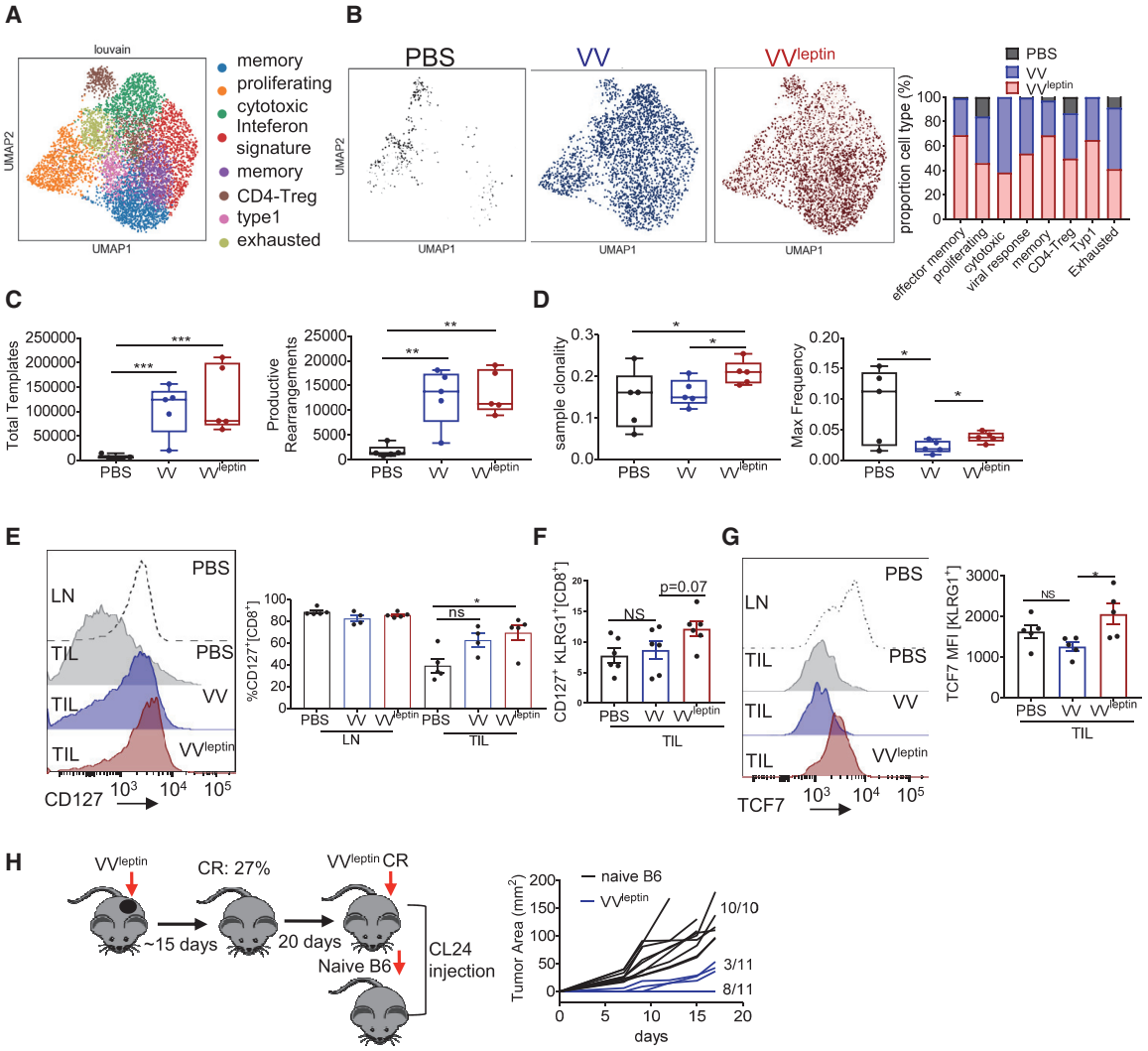

Figure 6. Leptin Promotes Memory Responses in the Oncolytic Virus-Induced Immune Infiltrate

C57BL/6J mice were injected subdermally with CL24 cells. Tumors were treated intratumorally with PBS, VV, or VV^{leptin} 5–7 days after tumor cell injection.

(A) Unsupervised clustering within T cells (scRNA-seq) from PBS-, VV, and VV^{leptin}-treated tumor infiltrate.

(B) Comparison of T cell population between PBS, VV, and VV^{leptin} treatment. Quantification of the proportion of each cell-type population based on treatment is shown. On day 10 after treatment, lymphocytes were isolated from tumor-infiltrating lyphocytes (TILs) and LNs.

(C) TCR sequencing of genomic DNA extracted from CL24-bearing mice treated intratumorally with PBS, VV, or VV^{leptin} at 2.5 × 10^6 PFU (n = 5 each treatment). Analysis of total templates and productive rearrangements is shown.

(D) Analysis of sample clonality and mean frequency.

(E–G) Mice were treated as in (A). Representative histograms and tabulated flow cytometric data of CD8$^+$ T cells stained for CD127 expression (E), CD127 with KLRG1 expression (F), and TCF7 expression in KLRG1$^+$ population (G) are shown.

(H) Mice were treated as in (A). Complete responders from VV^{leptin} treatment of CL24 tumors (n = 11) and naive mice (n = 10) received an injection of CL24 cells and were monitored for tumor growth.

Data represent at least three independent experiments. *p < 0.05, **p < 0.01, and ***p < 0.001 by two-way ANOVA. Error bars indicate SEMs. See also Figures S5 and S6.

to the microenvironment, consequently improving therapeutic efficacy. Recent studies have started to explore the genetic signature defined by oncolytic viruses in the tumor and determining targets that can be expressed in oncolytic viruses (Zamarin et al., 2017). The present study detailed the changes in the immune landscape after oncolytic viral treatments using scRNA-seq analysis. Our findings reveal changes in tumor infiltrate at an early time point, when tumors are not yet regressing. These data suggest that oncolytic viruses do not simply lyse a portion of tumor cells and promote some immunogenic cell death, but rather have the capacity to completely remodel the tumor immune microenvironment. This remodeling promotes the infiltration of new T cells that are sensitive to signals that may influence their fate toward dysfunction or memory. Our data show not only an increased infiltration in the T cell compartment, which is likely central to the antitumor immunity we observe, but also a

wide array of changes in the myeloid population, particularly in the macrophage compartment. A better understanding of the classification of macrophages and their function would be critical to dissect their role in the response to oncolytic viruses. What is unclear is whether these are a consequence of new T cell immunity, viral infection, or the tissue damage induced by oncolysis. Our study sheds light on the potent immunity induced by oncolytic viruses and suggests that this immune response can be bolstered in specific ways to promote more durable responses.

There is increasing evidence showing that improving T cell metabolic function in the tumor microenvironment allows for a better therapeutic response (Rivadeneira and Delgoffe, 2018). This study used leptin therapeutically as a metabolic modulator of the immune response, especially in cancer. Looking closely at the T cell compartment by scRNA-seq or flow cytometry analysis, we observed clear differences between the two viruses presented here, most notably the concept that providing induced increased metabolic capacity in T cells resulted in improved function and differentiation toward a memory-like phenotype, which are essential for durable responses. These complete responders develop a full memory response, preventing tumor regression when encountering a second tumor cell challenge. Thus, this new immunity induced in response to oncolytic viruses is not dominated by virus-specific clones, but rather contains potent, tumor-specific T cells that can prevent future tumor encounters. Furthermore, we highlight the potential for using oncolytic viruses as an effective delivery system for molecules that can modulate specifically the tumor microenvironment and improve the therapeutic response.

Previous studies have shown that immune cells express the leptin receptor (Procaccini et al., 2012) and that leptin as a cytokine can have pro-inflammatory functions in innate and adaptive immune responses (La Cava and Matarese, 2004; Loffreda et al., 1998; Santos-Alvarez et al., 1999). Regarding the adaptive immune response, leptin can activate and enhance the proliferation of human T lymphocytes (Martín-Romero et al., 2000). There are some observations that leptin may inhibit regulatory T cell proliferation and function in models of inflammation and autoimmunity (Feuerer et al., 2009; Matarese et al., 2001). Our data using oncolytics suggest that T_{reg} cells are certainly not stimulated in a leptin-rich tumor environment, although it remains unclear whether they are functionally inhibited when leptin is overexpressed.

Little is known about the role of leptin or the leptin receptor in cancer, particularly in the tumor microenvironment. Our findings demonstrate that there is an increase leptin receptor expression in T cells in the tumor microenvironment compared to those in the secondary lymphoid organs. Leptin can metabolically enhance tumor-infiltrating T cell effector function through the persistence of mitochondrial function and an increase in oxidative phosphorylation. Previous studies have introduced the concept that leptin can have a direct metabolic effect by promoting fatty acid oxidation in skeletal muscle (Steinberg et al., 2002). In the context of immune cells, $CD4^+$ T cells from leptin-deficient mice show a reduction in glucose uptake along with decreased proliferation and cytokine production (Saucillo et al., 2014). It is important to note that previous studies of leptin-induced changes in T cell metabolism are conducted in the context of obesity or fasting (Gerriets et al., 2016; Saucillo et al., 2014). Our data suggest that T cells that are "starved" in the nutrient dearth tumor microenvironment may be ideal targets for metabolic mediators such as leptin. Our data reinforce previous studies showing that leptin signals through the activation of important signaling pathways such as p38-MAPK and STAT3 (Ghilardi and Skoda, 1997; Niswender et al., 2001; Papathanassoglou et al., 2006) and can increase mitochondrial content and quality. Leptin can promote peroxisome proliferator-activated receptor γ co-activator 1α (PGC-1α) activation and promote oxidative phosphorylation as well as promote mitochondrial fusion through the expression of mitofusin 1 (Hsu et al., 2015; Roman et al., 2010). As we have previously shown that tumor-infiltrating T cells repress the expression of PGC-1α (Scharping et al., 2016), leptin may support tumor-infiltrating lymphocyte function through the maintenance of that axis.

Our analysis of the T cell infiltration of both wild-type and leptin-engineered oncolytic *Vaccinia* shed light on the immune populations that were predominant in the tumors treated with leptin-expressing *Vaccinia* virus. We found an increase in the proportions of memory T cells, which can explain the sustained therapeutic response observed. Memory T cells are superior antitumor T cells and have a higher mitochondrial content and oxidative phosphorylation capacity (Sukumar et al., 2016; van der Windt et al., 2012), in accordance with our data showing an increase in mitochondrial content. TCR sequencing analysis further expanded our understanding of the effects of oncolytic viruses on tumor-infiltrating lymphocytes. While oncolytics predictably induced new T cell clones to infiltrate the tumor, we observed a T cell clonal expansion in tumors treated with leptin-expressing *Vaccinia* virus. Our TRP2-tetramer data highlight the notion that the new T cell infiltrate is potentially recognizing new antigens and therefore the TRP2-specific population is underrepresented. While our data using tumor rechallenge suggest that at least a portion of these T cells are tumor specific, further studies could determine the antigen specificity of these clones and how important these clones are for therapeutic response.

Our work and that of others have shown the benefits of metabolically enhancing mitochondrial function in tumor-infiltrating lymphocytes. Our study opens up the possibility of further expanding the repertoire of metabolic modulators, among the myriad encoded in the genome that can be delivered directly into the tumor. An attractive method of therapeutic delivery of these metabolic modulators is the utilization of oncolytic viruses, which can deliver a genetically encoded payload directly to the tumor microenvironment. Until now, the majority of oncolytic-delivered genes have been immunologic in nature (e.g., cytokines, co-stimulatory molecules). However, our study represents a proof of concept that metabolic modulators can be delivered by oncolytic viruses. While we chose *Vaccinia* for its distinct characteristics, our data suggest that these modalities may be broadly applicable and encoded in other oncolytics such as herpes simplex virus (HSV), Newcastle disease virus, adenovirus (NDV), and vesicular stomatitis virus (VSV). Furthermore, testing *Vaccinia* and other oncolytic models in systemic delivery would be of great interest for future studies, particularly in tumor models in which intratumoral injections are not viable or in the treatment

of distant metastases. While our scRNA-seq revealed that oncolytics have potent immunostimulatory potential early after infection, it is clear that to achieve durable, complete responses, metabolic support is crucial and may help guide the strong early effector response into long-lived memory capable of mediating robust antitumor effects.

STAR★METHODS

Detailed methods are provided in the online version of this paper and include the following:

- KEY RESOURCES TABLE
- LEAD CONTACT AND MATERIALS AVAILABILITY
- EXPERIMENTAL MODEL AND SUBJECT DETAILS
  - Mice
  - Cell culture
- METHOD DETAILS
  - Tumor models
  - Oncolytic virus production
  - T cell isolations from lymph node, tumor, and adoptive transfer
  - Metabolic Assays
  - Immunoblotting
  - ELISA
  - TCR Sequencing
  - Single cell RNA sequencing analysis
- QUANTIFICATION AND STATISTICAL ANALYSIS
- DATA AND CODE AVAILABILITY

SUPPLEMENTAL INFORMATION

Supplemental Information can be found online at https://doi.org/10.1016/j.immuni.2019.07.003.

ACKNOWLEDGMENTS

The authors thank Nicole Scharping for technical and mentoring assistance and Dr. Chandranath Roy for assistance with virus production. This work was primarily supported by a Stand Up to Cancer Innovative Research Grant (SU2C-AACR-IRG-04-16) and was additionally supported by the NIH Director's New Innovator Award (DP2AI136598) to G.M.D., the UPMC Hillman Cancer Center Melanoma and Skin Cancer SPORE (P50CA121973-09) to G.M.D., the Head and Neck Cancer SPORE (P50CA097190) to R.L.F. and G.M.D., the Alliance for Cancer Gene Therapy/Swim Across America to G.M.D., and the Sy Holzer Endowed Immunotherapy Fund to G.M.D.

AUTHOR CONTRIBUTIONS

D.B.R. performed experiments and data analysis and contributed to the preparation of the manuscript. A.V.M. performed the metabolic flux analysis experiments and generated the CL24 cell line. K.D. and Y.W. assisted with the *in vivo* experiments and analysis. A.K., T.T., and R.L. contributed to the analysis of the single-cell RNA sequencing data. R.L.F. helped oversee the research and provided scientific direction. P.S., S.N.S., and S.H.T. contributed to the acquisition, cloning, and generation of *Vaccinia* virus used in this project. G.M.D. conceived of and oversaw the research, analyzed the data, obtained research funding, and wrote the manuscript.

DECLARATION OF INTERESTS

The use of metabolic-reprogramming oncolytic viruses is the subject of a patent application on which D.B.R., P.S., S.H.T., and G.M.D. are listed as inventors. P.S. and S.H.T. are employees of Western Oncolytics.

Received: October 19, 2018
Revised: May 16, 2019
Accepted: July 12, 2019
Published: August 27, 2019

REFERENCES

Abella, V., Scotece, M., Conde, J., Pino, J., Gonzalez-Gay, M.A., Gómez-Reino, J.J., Mera, A., Lago, F., Gómez, R., and Gualillo, O. (2017). Leptin in the interplay of inflammation, metabolism and immune system disorders. Nat. Rev. Rheumatol. *13*, 100–109.

Akimoto, T., Pohnert, S.C., Li, P., Zhang, M., Gumbs, C., Rosenberg, P.B., Williams, R.S., and Yan, Z. (2005). Exercise stimulates Pgc-1alpha transcription in skeletal muscle through activation of the p38 MAPK pathway. J. Biol. Chem. *280*, 19587–19593.

Andtbacka, R.H., Kaufman, H.L., Collichio, F., Amatruda, T., Senzer, N., Chesney, J., Delman, K.A., Spitler, L.E., Puzanov, I., Agarwala, S.S., et al. (2015). Talimogene Laherparepvec Improves Durable Response Rate in Patients With Advanced Melanoma. J. Clin. Oncol. *33*, 2780–2788.

Barve, M., Bender, J., Senzer, N., Cunningham, C., Greco, F.A., McCune, D., Steis, R., Khong, H., Richards, D., Stephenson, J., et al. (2008). Induction of immune responses and clinical efficacy in a phase II trial of IDM-2101, a 10-epitope cytotoxic T-lymphocyte vaccine, in metastatic non-small-cell lung cancer. J. Clin. Oncol. *26*, 4418–4425.

Brown, M.C., Holl, E.K., Boczkowski, D., Dobrikova, E., Mosaheb, M., Chandramohan, V., Bigner, D.D., Gromeier, M., and Nair, S.K. (2017). Cancer immunotherapy with recombinant poliovirus induces IFN-dominant activation of dendritic cells and tumor antigen-specific CTLs. Sci. Transl. Med. *9*, eaan4220.

Buller, R.M., Smith, G.L., Cremer, K., Notkins, A.L., and Moss, B. (1985). Decreased virulence of recombinant vaccinia virus expression vectors is associated with a thymidine kinase-negative phenotype. Nature *317*, 813–815.

Chang, C.H., Qiu, J., O'Sullivan, D., Buck, M.D., Noguchi, T., Curtis, J.D., Chen, Q., Gindin, M., Gubin, M.M., van der Windt, G.J., et al. (2015). Metabolic Competition in the Tumor Microenvironment Is a Driver of Cancer Progression. Cell *162*, 1229–1241.

Coleman, D.L. (1979). Obesity genes: beneficial effects in heterozygous mice. Science *203*, 663–665.

Dankort, D., Curley, D.P., Cartlidge, R.A., Nelson, B., Karnezis, A.N., Damsky, W.E., Jr., You, M.J., DePinho, R.A., McMahon, M., and Bosenberg, M. (2009). Braf(V600E) cooperates with Pten loss to induce metastatic melanoma. Nat. Genet. *41*, 544–552.

De Rosa, V., Procaccini, C., Calì, G., Pirozzi, G., Fontana, S., Zappacosta, S., La Cava, A., and Matarese, G. (2007). A key role of leptin in the control of regulatory T cell proliferation. Immunity *26*, 241–255.

Delgoffe, G.M., Kole, T.P., Cotter, R.J., and Powell, J.D. (2009). Enhanced interaction between Hsp90 and raptor regulates mTOR signaling upon T cell activation. Mol. Immunol. *46*, 2694–2698.

Dixit, V.D., Schaffer, E.M., Pyle, R.S., Collins, G.D., Sakthivel, S.K., Palaniappan, R., Lillard, J.W., Jr., and Taub, D.D. (2004). Ghrelin inhibits leptin- and activation-induced proinflammatory cytokine expression by human monocytes and T cells. J. Clin. Invest. *114*, 57–66.

Feuerer, M., Herrero, L., Cipolletta, D., Naaz, A., Wong, J., Nayer, A., Lee, J., Goldfine, A.B., Benoist, C., Shoelson, S., and Mathis, D. (2009). Lean, but not obese, fat is enriched for a unique population of regulatory T cells that affect metabolic parameters. Nat. Med. *15*, 930–939.

Friedman, G.K., Haas, M.C., Kelly, V.M., Markert, J.M., Gillespie, G.Y., and Cassady, K.A. (2012). Hypoxia Moderates γ(1)34.5-Deleted Herpes Simplex Virus Oncolytic Activity in Human Glioma Xenoline Primary Cultures. Transl. Oncol. *5*, 200–207.

Gerriets, V.A., Danzaki, K., Kishton, R.J., Eisner, W., Nichols, A.G., Saucillo, D.C., Shinohara, M.L., and MacIver, N.J. (2016). Leptin directly promotes T-cell glycolytic metabolism to drive effector T-cell differentiation in a mouse model of autoimmunity. Eur. J. Immunol. *46*, 1970–1983.

Ghilardi, N., and Skoda, R.C. (1997). The leptin receptor activates janus kinase 2 and signals for proliferation in a factor-dependent cell line. Mol. Endocrinol. *11*, 393–399.

Herbst, R.S., Soria, J.C., Kowanetz, M., Fine, G.D., Hamid, O., Gordon, M.S., Sosman, J.A., McDermott, D.F., Powderly, J.D., Gettinger, S.N., et al. (2014). Predictive correlates of response to the anti-PD-L1 antibody MPDL3280A in cancer patients. Nature *515*, 563–567.

Hiley, C.T., Yuan, M., Lemoine, N.R., and Wang, Y. (2010). Lister strain vaccinia virus, a potential therapeutic vector targeting hypoxic tumours. Gene Ther. *17*, 281–287.

Ho, P.C., Bihuniak, J.D., Macintyre, A.N., Staron, M., Liu, X., Amezquita, R., Tsui, Y.C., Cui, G., Micevic, G., Perales, J.C., et al. (2015). Phosphoenolpyruvate Is a Metabolic Checkpoint of Anti-tumor T Cell Responses. Cell *162*, 1217–1228.

Howard, J.K., Lord, G.M., Matarese, G., Vendetti, S., Ghatei, M.A., Ritter, M.A., Lechler, R.I., and Bloom, S.R. (1999). Leptin protects mice from starvation-induced lymphoid atrophy and increases thymic cellularity in ob/ob mice. J. Clin. Invest. *104*, 1051–1059.

Hsu, W.H., Lee, B.H., and Pan, T.M. (2015). Leptin-induced mitochondrial fusion mediates hepatic lipid accumulation. Int. J. Obes. *39*, 1750–1756.

Justus, C.R., Sanderlin, E.J., and Yang, L.V. (2015). Molecular Connections between Cancer Cell Metabolism and the Tumor Microenvironment. Int. J. Mol. Sci. *16*, 11055–11086.

Kanerva, A., Nokisalmi, P., Diaconu, I., Koski, A., Cerullo, V., Liikanen, I., Tähtinen, S., Oksanen, M., Heiskanen, R., Pesonen, S., et al. (2013). Antiviral and antitumor T-cell immunity in patients treated with GM-CSF-coding oncolytic adenovirus. Clin. Cancer Res. *19*, 2734–2744.

Kirn, D.H., Wang, Y., Le Boeuf, F., Bell, J., and Thorne, S.H. (2007). Targeting of interferon-beta to produce a specific, multi-mechanistic oncolytic vaccinia virus. PLoS Med. *4*, e353.

Klingenberg, R., Lebens, M., Hermansson, A., Fredrikson, G.N., Strodthoff, D., Rudling, M., Ketelhuth, D.F., Gerdes, N., Holmgren, J., Nilsson, J., and Hansson, G.K. (2010). Intranasal immunization with an apolipoprotein B-100 fusion protein induces antigen-specific regulatory T cells and reduces atherosclerosis. Arterioscler. Thromb. Vasc. Biol. *30*, 946–952.

La-Beck, N.M., Jean, G.W., Huynh, C., Alzghari, S.K., and Lowe, D.B. (2015). Immune Checkpoint Inhibitors: New Insights and Current Place in Cancer Therapy. Pharmacotherapy *35*, 963–976.

La Cava, A., and Matarese, G. (2004). The weight of leptin in immunity. Nat. Rev. Immunol. *4*, 371–379.

Loffreda, S., Yang, S.Q., Lin, H.Z., Karp, C.L., Brengman, M.L., Wang, D.J., Klein, A.S., Bulkley, G.B., Bao, C., Noble, P.W., et al. (1998). Leptin regulates proinflammatory immune responses. FASEB J. *12*, 57–65.

Lord, G.M., Matarese, G., Howard, J.K., Baker, R.J., Bloom, S.R., and Lechler, R.I. (1998). Leptin modulates the T-cell immune response and reverses starvation-induced immunosuppression. Nature *394*, 897–901.

Mahoney, K.M., Rennert, P.D., and Freeman, G.J. (2015). Combination cancer immunotherapy and new immunomodulatory targets. Nat. Rev. Drug Discov. *14*, 561–584.

Martín-Romero, C., Santos-Alvarez, J., Goberna, R., and Sánchez-Margalet, V. (2000). Human leptin enhances activation and proliferation of human circulating T lymphocytes. Cell. Immunol. *199*, 15–24.

Matarese, G., Di Giacomo, A., Sanna, V., Lord, G.M., Howard, J.K., Di Tuoro, A., Bloom, S.R., Lechler, R.I., Zappacosta, S., and Fontana, S. (2001). Requirement for leptin in the induction and progression of autoimmune encephalomyelitis. J. Immunol. *166*, 5909–5916.

Menk, A.V., Scharping, N.E., Rivadeneira, D.B., Calderon, M.J., Watson, M.J., Dunstane, D., Watkins, S.C., and Delgoffe, G.M. (2018). 4-1BB costimulation induces T cell mitochondrial function and biogenesis enabling cancer immunotherapeutic responses. J. Exp. Med. *215*, 1091–1100.

Moss, B. (2013). Poxvirus DNA replication. Cold Spring Harb. Perspect. Biol. *5*, a010199.

Najjar, Y.G., Menk, A.V., Sander, C., Rao, U., Karunamurthy, A., Bhatia, R., Zhai, S., Kirkwood, J.M., and Delgoffe, G.M. (2019). Tumor cell oxidative metabolism as a barrier to PD-1 blockade immunotherapy in melanoma. JCI Insight *4*, 124989.

Niswender, K.D., Morton, G.J., Stearns, W.H., Rhodes, C.J., Myers, M.G., Jr., and Schwartz, M.W. (2001). Intracellular signalling. Key enzyme in leptin-induced anorexia. Nature *413*, 794–795.

Papathanassoglou, E., El-Haschimi, K., Li, X.C., Matarese, G., Strom, T., and Mantzoros, C. (2006). Leptin receptor expression and signaling in lymphocytes: kinetics during lymphocyte activation, role in lymphocyte survival, and response to high fat diet in mice. J. Immunol. *176*, 7745–7752.

Pérez-Pérez, A., Vilariño-García, T., Fernández-Riejos, P., Martín-González, J., Segura-Egea, J.J., and Sánchez-Margalet, V. (2017). Role of leptin as a link between metabolism and the immune system. Cytokine Growth Factor Rev. *35*, 71–84.

Pipiya, T., Sauthoff, H., Huang, Y.Q., Chang, B., Cheng, J., Heitner, S., Chen, S., Rom, W.N., and Hay, J.G. (2005). Hypoxia reduces adenoviral replication in cancer cells by downregulation of viral protein expression. Gene Ther. *12*, 911–917.

Procaccini, C., Jirillo, E., and Matarese, G. (2012). Leptin as an immunomodulator. Mol. Aspects Med. *33*, 35–45.

Puhlmann, M., Brown, C.K., Gnant, M., Huang, J., Libutti, S.K., Alexander, H.R., and Bartlett, D.L. (2000). Vaccinia as a vector for tumor-directed gene therapy: biodistribution of a thymidine kinase-deleted mutant. Cancer Gene Ther. *7*, 66–73.

Ricca, J.M., Oseledchyk, A., Walther, T., Liu, C., Mangarin, L., Merghoub, T., Wolchok, J.D., and Zamarin, D. (2018). Pre-existing Immunity to Oncolytic Virus Potentiates Its Immunotherapeutic Efficacy. Mol. Ther. *26*, 1008–1019.

Rivadeneira, D.B., and Delgoffe, G.M. (2018). Antitumor T-cell Reconditioning: Improving Metabolic Fitness for Optimal Cancer Immunotherapy. Clin. Cancer Res. *24*, 2473–2481.

Robins, H.S., Campregher, P.V., Srivastava, S.K., Wacher, A., Turtle, C.J., Kahsai, O., Riddell, S.R., Warren, E.H., and Carlson, C.S. (2009). Comprehensive assessment of T-cell receptor beta-chain diversity in alpha-beta T cells. Blood *114*, 4099–4107.

Roman, E.A., Reis, D., Romanatto, T., Maimoni, D., Ferreira, E.A., Santos, G.A., Torsoni, A.S., Velloso, L.A., and Torsoni, M.A. (2010). Central leptin action improves skeletal muscle AKT, AMPK, and PGC1 alpha activation by hypothalamic PI3K-dependent mechanism. Mol. Cell. Endocrinol. *314*, 62–69.

Russell, S.J., and Barber, G.N. (2018). Oncolytic Viruses as Antigen-Agnostic Cancer Vaccines. Cancer Cell *33*, 599–605.

Sanchez-Margalet, V., and Martin-Romero, C. (2001). Human leptin signaling in human peripheral blood mononuclear cells: activation of the JAK-STAT pathway. Cell. Immunol. *211*, 30–36.

Santos-Alvarez, J., Goberna, R., and Sánchez-Margalet, V. (1999). Human leptin stimulates proliferation and activation of human circulating monocytes. Cell. Immunol. *194*, 6–11.

Saucillo, D.C., Gerriets, V.A., Sheng, J., Rathmell, J.C., and Maciver, N.J. (2014). Leptin metabolically licenses T cells for activation to link nutrition and immunity. J. Immunol. *192*, 136–144.

Scharping, N.E., Menk, A.V., Moreci, R.S., Whetstone, R.D., Dadey, R.E., Watkins, S.C., Ferris, R.L., and Delgoffe, G.M. (2016). The Tumor Microenvironment Represses T Cell Mitochondrial Biogenesis to Drive Intratumoral T Cell Metabolic Insufficiency and Dysfunction. Immunity *45*, 701–703.

Scharping, N.E., Menk, A.V., Whetstone, R.D., Zeng, X., and Delgoffe, G.M. (2017). Efficacy of PD-1 Blockade Is Potentiated by Metformin-Induced Reduction of Tumor Hypoxia. Cancer Immunol. Res. *5*, 9–16.

Sharma, P., Hu-Lieskovan, S., Wargo, J.A., and Ribas, A. (2017). Primary, Adaptive, and Acquired Resistance to Cancer Immunotherapy. Cell *168*, 707–723.

Siska, P.J., and Rathmell, J.C. (2015). T cell metabolic fitness in antitumor immunity. Trends Immunol. *36*, 257–264.

Steinberg, G.R., Parolin, M.L., Heigenhauser, G.J., and Dyck, D.J. (2002). Leptin increases FA oxidation in lean but not obese human skeletal muscle:

evidence of peripheral leptin resistance. Am. J. Physiol. Endocrinol. Metab. *283*, E187–E192.

Sukumar, M., Liu, J., Mehta, G.U., Patel, S.J., Roychoudhuri, R., Crompton, J.G., Klebanoff, C.A., Ji, Y., Li, P., Yu, Z., et al. (2016). Mitochondrial Membrane Potential Identifies Cells with Enhanced Stemness for Cellular Therapy. Cell Metab. *23*, 63–76.

van der Windt, G.J., Everts, B., Chang, C.H., Curtis, J.D., Freitas, T.C., Amiel, E., Pearce, E.J., and Pearce, E.L. (2012). Mitochondrial respiratory capacity is a critical regulator of CD8+ T cell memory development. Immunity *36*, 68–78.

van der Windt, G.J.W., O'Sullivan, D., Everts, B., Huang, S.C.-C., Buck, M.D., Curtis, J.D., Chang, C.-H., Smith, A.M., Ai, T., Faubert, B., et al. (2013). CD8 memory T cells have a bioenergetic advantage that underlies their rapid recall ability. Proc. Natl. Acad. Sci. USA *110*, 14336–14341.

Wang, Z., Aguilar, E.G., Luna, J.I., Dunai, C., Khuat, L.T., Le, C.T., Mirsoian, A., Minnar, C.M., Stoffel, K.M., Sturgill, I.R., et al. (2019). Paradoxical effects of obesity on T cell function during tumor progression and PD-1 checkpoint blockade. Nat. Med. *25*, 141–151.

Weber, J.S., D'Angelo, S.P., Minor, D., Hodi, F.S., Gutzmer, R., Neyns, B., Hoeller, C., Khushalani, N.I., Miller, W.H., Jr., Lao, C.D., et al. (2015). Nivolumab versus chemotherapy in patients with advanced melanoma who progressed after anti-CTLA-4 treatment (CheckMate 037): a randomised, controlled, open-label, phase 3 trial. Lancet Oncol. *16*, 375–384.

Whitman, E.D., Tsung, K., Paxson, J., and Norton, J.A. (1994). In vitro and in vivo kinetics of recombinant vaccinia virus cancer-gene therapy. Surgery *116*, 183–188.

Wolf, F.A., Angerer, P., and Theis, F.J. (2018). SCANPY: large-scale single-cell gene expression data analysis. Genome Biol. *19*, 15.

Zamarin, D., Holmgaard, R.B., Ricca, J., Plitt, T., Palese, P., Sharma, P., Merghoub, T., Wolchok, J.D., and Allison, J.P. (2017). Intratumoral modulation of the inducible co-stimulator ICOS by recombinant oncolytic virus promotes systemic anti-tumour immunity. Nat. Commun. *8*, 14340.

Zhou, X., Yu, S., Zhao, D.M., Harty, J.T., Badovinac, V.P., and Xue, H.H. (2010). Differentiation and persistence of memory CD8(+) T cells depend on T cell factor 1. Immunity *33*, 229–240.

STAR★METHODS

KEY RESOURCES TABLE

REAGENT or RESOURCE	SOURCE	IDENTIFIER
Antibodies		
B220-PerCP Cy5.5 (monoclonal)	Biolegend	Cat# 103236; RRID: AB_893354
TNFα PerCP Cy5.5 (monoclonal)	Biolegend	Cat# 506322; RRID: AB_961434
CD4 PerCP Cy5.5 (monoclonal)	Biolegend	Cat# 100433; RRID: AB_893330
VDAC AF488 (monoclonal)	Abcam	Cat# ab179839
IFNγ BV510 (monoclonal)	Biolegend	Cat# 505842; RRID: AB_2734494
PD1 BV786 (monoclonal)	Biolegend	Cat#135225; RRID: AB_2563680
NK1.1 APC (monoclonal)	BD pharmigen	Cat# 561117; RRID: AB_10563422
Tim3 PE (monoclonal)	Biolegend	Cat# 119703; RRID: AB_345377
Ki67 BV605 (monoclonal)	Biolegend	Cat# 652413; RRID: AB_2562664
p-p38MAPK (T180/Y182) – PE (monoclonal)	Cell Signaling	Cat# 6908S; RRID: AB_10839411
p-NF-kappaB p65 (S536) - A647 (monoclonal)	Cell Signaling	Cat# 4887S; RRID: AB_561198
pSTAT3 (Tyr705) BV421 (monoclonal)	Biolegend	Cat# 651009; RRID: AB_2572087
CD127 (IL7Ra) PE- Cy7 (monoclonal)	Biolegend	Cat# 135014; RRID: AB_1937265
CD62L BV786 (monoclonal)	BD Horizon	Cat# 564109; RRID: AB_2738598
KLRG1 APC-Cy7 (monoclonal)	Biolegend	Cat# 138426; RRID: AB_2566554
TCF7/TCF1 FITC (monoclonal)	R&D systems	Cat# IC8224G
Foxp3 AxF700 (monoclonal)	Thermo Fisher	Cat# 56-5773-82; RRID: AB_1210557
Leptin R biotinylated (mouse polyclonal)	R&D systems	Cat# BAF497; RRID: AB_2296953
Mouse Leptin (polyclonal Goat)	R&D systems	Cat # AF498; RRID: AB_355394
Phospho- ATF-2 (Thr71) (rabbit monoclonal)	Cell Signaling	Cat# 24329
P38 MAPK (rabbit monoclonal)	Cell Signaling	Cat# 9212S; RRID: AB_330713
InVivo Mab Anti-mouse CD8α(YTS 169.4)	BioXCell	BE0117; RRID: AB_10950145
InVivoMAb rat IgG1 Isotype control	BioXCell	BE0290; RRID: AB_2687813
β-Actin (C4) (mouse monoclonal)	Santa Cruz	Cat# SC-47778; RRID: AB_2714189
Bacterial and Virus Strains		
wild-type *Vaccinia* virus Western Reserve (WR)	American Type Culture Collection (BEI Resources)	Cat# NR2639
One Shot® Stbl3 Chemically Competent *E. coli*	Fisher	Cat# C737303
Chemicals, Peptides, and Recombinant Proteins		
2NBDG	Cayman Chemical	Cat# 186689-07-6
Mitotracker™ Deep Red FM	Invitrogen	Cat# M22426
Tetramer H-2Kb TRP-2 PE	MBL International	Cat# TB-5004-1
Tetramer VACV B8R BV421	MBL International	Cat# BTB-M538
Recombinant mouse Leptin	R&D systems	Cat# 498-OB-01M
L-glutamine	Fisher	Cat# MT25005CI
Oligomycin Complex	Cayman Chemical	Cat# 11341
FCCP	Cayman Chemical	Cat# 15218
2-deoxy-D-glucose (2DG)	Sigma	Cat# D8375-5G
Rotenone	Sigma	Cat# R8875-5G
Antimycin A	Sigma	Cat# A8674-25MG
Recombinant Murine IL-2	Peprotech	Cat# 212-12
SIINFEKL peptide	AnaSpec	Cat# AS-60193-1
Deposited Data		
Raw and analyzed data SC-RNaseq	This paper	GEO: GSE133699

(*Continued on next page*)

Continued		
REAGENT or RESOURCE	SOURCE	IDENTIFIER
Experimental Models: Cell Lines		
CL24	Najjar et al., 2019	N/A
MC38	Gift from Dr. Dario Vignali (University of Pittsburgh)	N/A
PanCO2	Gift from Dr. Michael Lotze (University of Pittsburgh)	N/A
Experimental Models: Organisms/Strains		
B6.129P2-Lepr^{tm1Rck}	Jackson Laboratory	Stock# 008327
Pten$^{f/f}$*Braf*^{V600E}*Tyr*$^{Cre.ER}$	Jackson Laboratory	Stock # 013590
B6.Cg-Tg(Cd4-cre)1Cwi/BfluJ	Jackson Laboratory	Stock # 022071
Recombinant DNA		
Mouse Leptin natural ORF mammalian (pPCMV3-mLEP)	Sino Biological Inc.	Cat# MG50442-UT
PCMV3-untagged Negative Control Vector	Sino Biological Inc.	Cat# CV011
pSC65 plasmid	Kind gift from Prof. Bernie Moss, NIH	N/A
Software and Algorithms		
GraphPad Prism	GraphPad Software, Inc	https://www.graphpad.com/demos/
BD FACS Diva Sotware	BD Biosciences	
FlowJo version 10	TreeStar, Ahsland Oregon	https://www.flowjo.com
Seahorse Wave Desktop Software	Agilent	https://www.graphpad.com/demos/
Cell Ranger	10X Genomics	https://support.10xgenomics.com/single-cell-gene-expression/software/pipelines/latest/what-is-cell-ranger
Scanpy	Wolf et al., 2018	https://github.com/theislab/scanpy
Critical Commercial Assays		
10X Genomics	10X Genomics, Pleasanton, CA	https://www.10xgenomics.com/
Seahorse XFe96 Analyzers	Agilent	https://www.agilent.com/en/products/cell-analysis/seahorse-analyzers/seahorse-xfe96-analyzer

LEAD CONTACT AND MATERIALS AVAILABILITY

Further information and requests for materials and resource will be fulfilled by the Lead Contact, Greg Delgoffe (gdelgoffe@pitt.edu).

EXPERIMENTAL MODEL AND SUBJECT DETAILS

Mice

C57/BL6 mice and *Pten*$^{f/f}$*Braf*^{V600E}*Tyr*$^{Cre.ER}$ mice were obtained from Jackson Laboratories and bred in house. Leptin receptor flox mice (ObR$^{Flox)}$ were obtained from The Jackson Laboratory. These mice were crossed to CD4 Cre expressing mice. These mice when used in experimental procedure were males and females between of 6-7 weeks old. Diet induced obesity (DIO) mice were obtained from The Jackson Laboratory and were all males. All animal work and protocols in the current study were approved by the University of Pittsburgh Institutional Animal Care and Use Committee, accredited by the AAALAC.

Cell culture

Tumor experiments were conducted using a single-cell clone derived from a melanoma tumor formed from a female *Pten*$^{f/f}$*Braf*^{V600E}*Tyr*$^{Cre.ER}$mouse painted with tamoxifen (CL24, described in Najjar et al., 2019). PanCO2, a male mouse pancreatic ductal adenocarcinoma cell line, was a kind gift from Dr. Michael Lotze's lab. MC38 is a male mouse colon adenocarcinoma cell line was a kind gift from Dr. Dario Vignali. CL24, PanCO2 and MC38 were all cultured in DMEM, supplemented with 10% FBS (v/v) at 37°C with 5% CO_2.The cDNA for leptin was obtained from OriGene and transfected into CL24 followed by hygromycin selection (an empty vector plasmid was used as a control). Single cell clones were selected and grown as cell line CL24^{hygro} for control plasmid and CL24^{leptin} for leptin expressing cell line.

METHOD DETAILS

Tumor models

C57BL/6J mice were injected with $CL24^{hygro}$ or $CL24^{leptin}$ melanoma cell line (250,000 cells intradermally) on day 0 and followed until tumors reach 15 mm in any direction. Tumors were measured every other day with digital calipers and tumor size was calculated by LxW.

Tumors (CL24, MC38 and PanCO2) were treated with PBS, VV^{ctrl} or VV^{leptin} ($2.5x10^6$ PFU) intratumorally when tumors reached approximately a $20mm^2$ and tumor growth was monitored until tumors treated with PBS reached 15mm in any direction. For CD8 depletion experiments mice were injected every other day starting at day 0 with anti-CD8 (YTS) at 200ug per mouse. On day 7 mice were injected with $CL24^{hygro}$ or $CL24^{leptin}$ melanoma cell line (250,000 cells intradermally) and followed until tumor reach 15mm in any direction.

On day 7 when tumors reached 5mm diameter, mice were treated with *Vaccinia* virus as previously described and were started on either 0.2mg anti– PD1 or hamster IgG isotype control (Bio X Cell), injected every other day days intraperitoneally. Cohorts were sacrificed when control mouse tumors reached 15 mm in any direction measured.

Oncolytic virus production

The wild-type *Vaccinia* virus Western Reserve (WR) strain was obtained from the American Type Culture Collection (BEI Resources). WR.TK−.Luc+ were described previously (Kirn et al., 2007) and were constructed for this work, with the pSC65 plasmid (from Dr. Bernie Moss, NIH) cloned to express firefly luciferase from the viral pSE/L promoter and mouse leptin (*Lep*) from the p7.5 promoter. This was recombined into the viral TK gene. *Vaccinia* virus expressing leptin was generated by cloning in the leptin gene using Gibson Cloning (New England BioLabs) into the *Vaccinia* plasmid. Leptin gene was cloned from a mouse leptin ORF mammalian expression plasmid (Sino Biological Inc.).

T cell isolations from lymph node, tumor, and adoptive transfer

Spleen and lymph node $CD8^+$ T cells were isolated from mice. Tissue was harvested, mechanically disrupted, and incubated with a biotinylated antibody cocktail consisting of antibodies (BioLegend) to B220, CD11b, CD11c, CD16/32, CD19, CD25, CD105, NK1.1, TCR$\gamma\delta$, and CD4. After a wash step, cells were incubated with streptavidin-coated magnetic nanoparticles (BioLegend). After washing, $CD8^+$ cells were isolated by applying a magnetic field and removing untouched cells. For adoptive transfer, T cells were generated by activating Pmel-1 x Thy1.1 mice with peptide and expanding cells for 5 days in IL-2. Pmel $CD8^+$ T cells were intravenously delivered (10^7) to mice bearing $CL24^{hygro}$ and $CL24^{leptin}$ tumors. Mice were then sacrificed and TIL analyzed.

To obtain single-cell suspensions of tumor infiltrating lymphocytes, tumor bearing mice were sacrificed and tumors were harvested. Excised, whole tumors were injected repeatedly using 20G needles with 2mg/mL collagenase type VI, 2U/mL hyluronidase (Dispase), and 10U/mL DNase I (Sigma) in buffered RPMI with 10% FBS and incubated for 30 min at 37°C. Tumors were then mechanically disrupted between frosted glass slides and filtered to remove particulates, then vortexed for 2 min. In many experiments (especially prior to sorting), tumor homogenates were debulked of tumor cells using CD105-biotin mediated magnetic depletion.

Metabolic Assays

T cell metabolic output was measured by Seahorse technology as previously described (Scharping et al., 2017). Briefly, 100,000 T cells were seeded into Cell-Tak-coated XFe96 plates in minimal unbuffered assay media containing 25 mM glucose, 2 mM glutamine, and 1 mM sodium pyruvate. Cells received sequential injections of 2 μM oligmycin, 2 μM FCCP, 10 mM 2-deoxyglucose, and 0.5 μM rotenone/antimycin A.

We assayed single-cell metabolic capacity by flow cytometry. Specifically, we utilized 2-NBD-glucose (Cayman Chemical) and MitoTracker FM dyes (ThermoFisher) to assay the propensity of cells to take up glucose or generate intermediates via their mitochondria. Nondraining and draining lymph node or tumor preparations were pulsed with 20 μM 2-NBDG in 5% FBS-containing media for 30 min at 37°C. Cells were surface stained and loaded with MitoTracker FM dyes to measure mitochondrial mass and function.

Immunoblotting

Immunoblotting was performed as previously described (Delgoffe et al., 2009). Briefly cells were lysed in 1% NP-40 lysis buffer. Cell lysates were then separated by SDS-PAGE using a 4%–12% Bio-Rad gels. Gels were then transferred to a polyvinylidene difluoride membrane and blocked in 5% milk in Tris-buffered saline 0.1%Tween-20 (TBST). Membrane was then incubated overnight at 4°C with primary antibodies diluted in blocking buffer. Membrane was incubated with secondary antibody (anti-mouse horseradish peroxidase, Jackson ImmunoResearch) in blocking buffer for 1 hour at room temperature and subsequently washed 3 times for 10 minutes with TBST. Protein was visualized by chemiluminescence by using Western Lightning (PerkinElmer). Mouse Leptin/OB antibody (R&D system BAF498), p-ATF2 (Cell Signaling), β-actin (Santa Cruz) and p38 MAPK (Cell Signaling).

ELISA

ELISA plate was coated with 50uL capture antibody (1:1000 in PBS) and put at 4°C overnight. The next day, the plate was washed 3 times with wash buffer (1L PBS + 0.05% Tween 20). Next, the plate was blocked with 200uL blocking buffer (200mL PBS + 1% BSA)

for 1 hour at room temperature. Samples were added (50ul) in blocking buffer to the wells together with Standard Curve samples, and the plate was incubated at room temperature for 2 hours. Secondary antibody was added (1:2000 in blocking buffer) and incubated at room temperature for 1 hour. After one hour HRP streptavidin (1:2000 in blocking buffer) was added to the plate and incubated at room temperature for 30 min. 40uL TMB substrate A and 40uL TMB substrate B were added to develop samples. Plate was read at 450 nm in a plate reader. Antibodies used for leptin Elisa experiment: the following antibodies were used for the assay: Capture Mouse Leptin/OB antibody (R&D systems AF498) and detection antibody Mouse Leptin/OB antibody (R&D system BAF498).

TCR Sequencing

CL24 tumors treated with PBS, VV^{ctrl} or VV^{leptin} were excised and processed for genomic DNA extraction (DNeasy QIAGEN kit). TCR sequencing was then performed following the immunoSEQ assay (Adaptive Biotechnologies) for immunosequencing of the complementarity-determining region 3 (CDR3) variable regions of T cell receptor-β chains (TCRβ) (Robins et al., 2009). Sequences were then filtered for the identification and quantification of abundance of unique TCRβCDR3 regions and compared across samples.

Single cell RNA sequencing analysis

CL24 tumors were treated with PBS, VV^{ctrl} or VV^{leptin} (2.5x106 PFU) intratumorally for 7 days. Tumor infiltrating lymphocytes were isolated and sorted for $CD45^+$ lymphocytes. $CD45^+$ cell were loaded into the Chromium instrument (10X Genomics, Pleasanton, CA), and the resulting barcoded cDNAs were used to construct libraries. The libraries from each sample were then processed for RNA sequencing. Cell-gene unique molecular identifier counting matrices were generated usigng the 10x Genomics CellRanger (v.2.1.1) pipeline. Quality control and normalization and analysis were done using Scanpy package (Wolf et al., 2018). After QC and normalization, the Louvain algorithm which is a part of the Scanpy package was used to cluster cells. Identities were assigned to cell types by using a combination of top expressed genes and canonical cell type marker genes.

QUANTIFICATION AND STATISTICAL ANALYSIS

All statistical analyses were performed using Prism 7 (GraphPad Software). Data were analyzed with the unpaired t test or one-way ANOVA with Tukey correction. Data are presented as mean ± SD * $p < 0.05$; ** $p < 0.01$; **** $p < 0.0001$; ns, not significant.

DATA AND CODE AVAILABILITY

The accession number for the RNA-seq data reported in this paper is GEO: GSE133699. All software used in the analysis is listed in the Key Resources Table.

Immunity, Volume *51*

Supplemental Information

Oncolytic Viruses Engineered to Enforce Leptin Expression Reprogram Tumor-Infiltrating T Cell Metabolism and Promote Tumor Clearance

Dayana B. Rivadeneira, Kristin DePeaux, Yiyang Wang, Aditi Kulkarni, Tracy Tabib, Ashley V. Menk, Padmavathi Sampath, Robert Lafyatis, Robert L. Ferris, Saumendra N. Sarkar, Stephen H. Thorne, and Greg M. Delgoffe

Figure S1

a

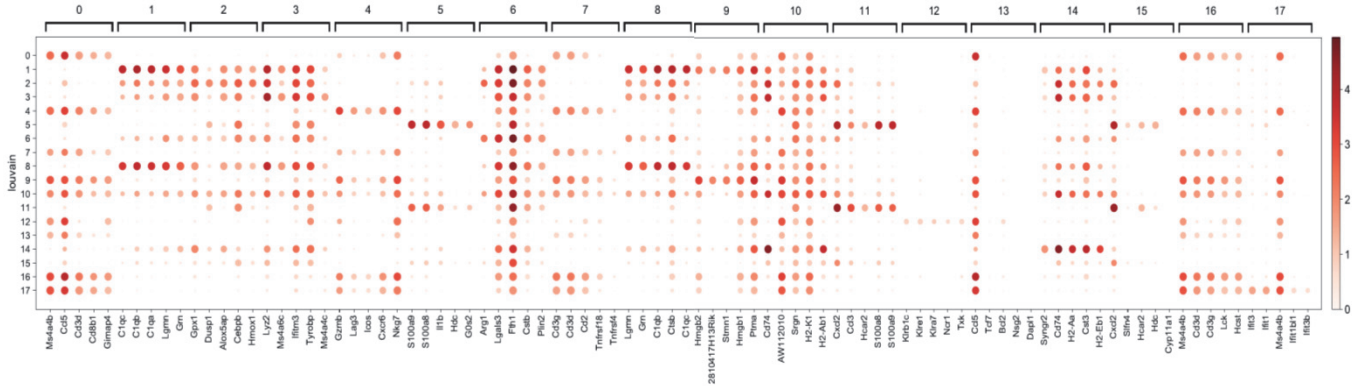

b

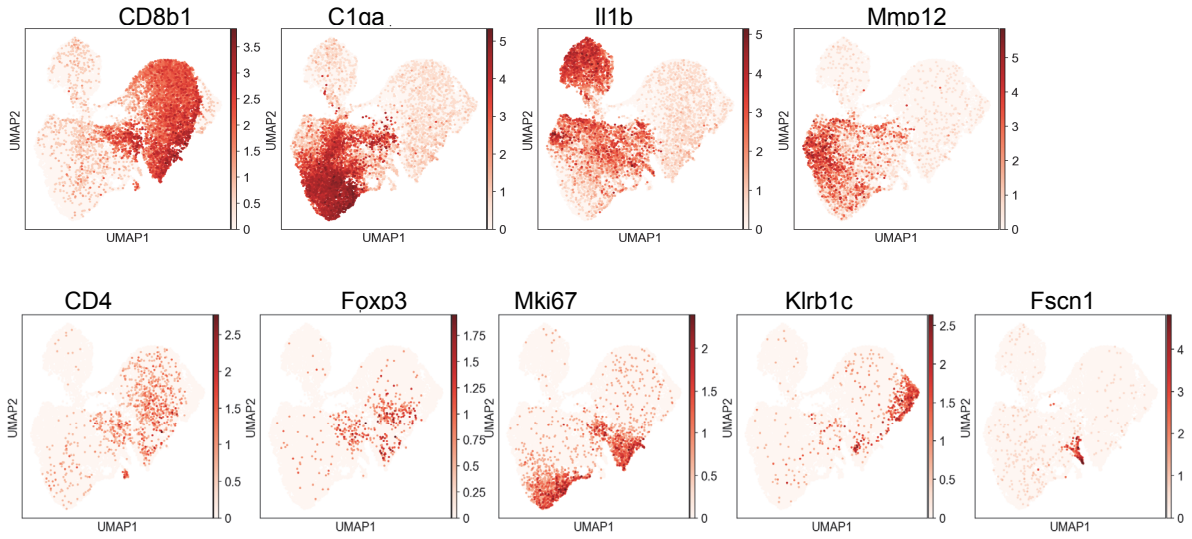

c

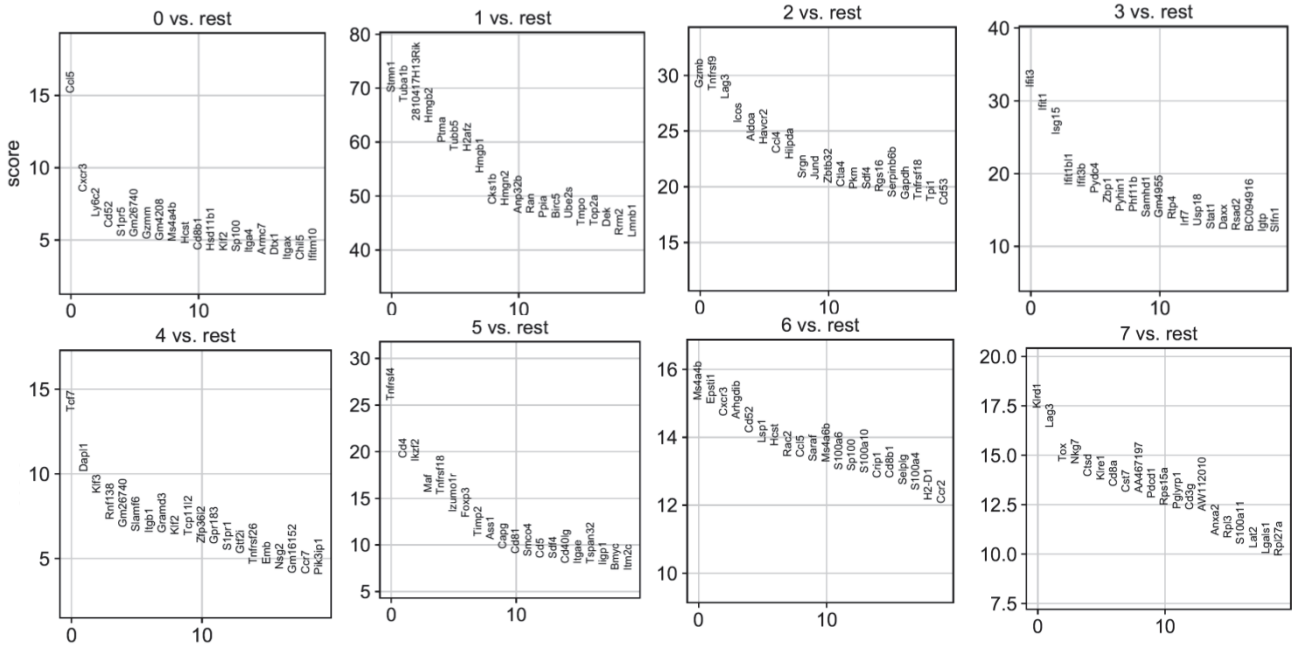

Figure S2

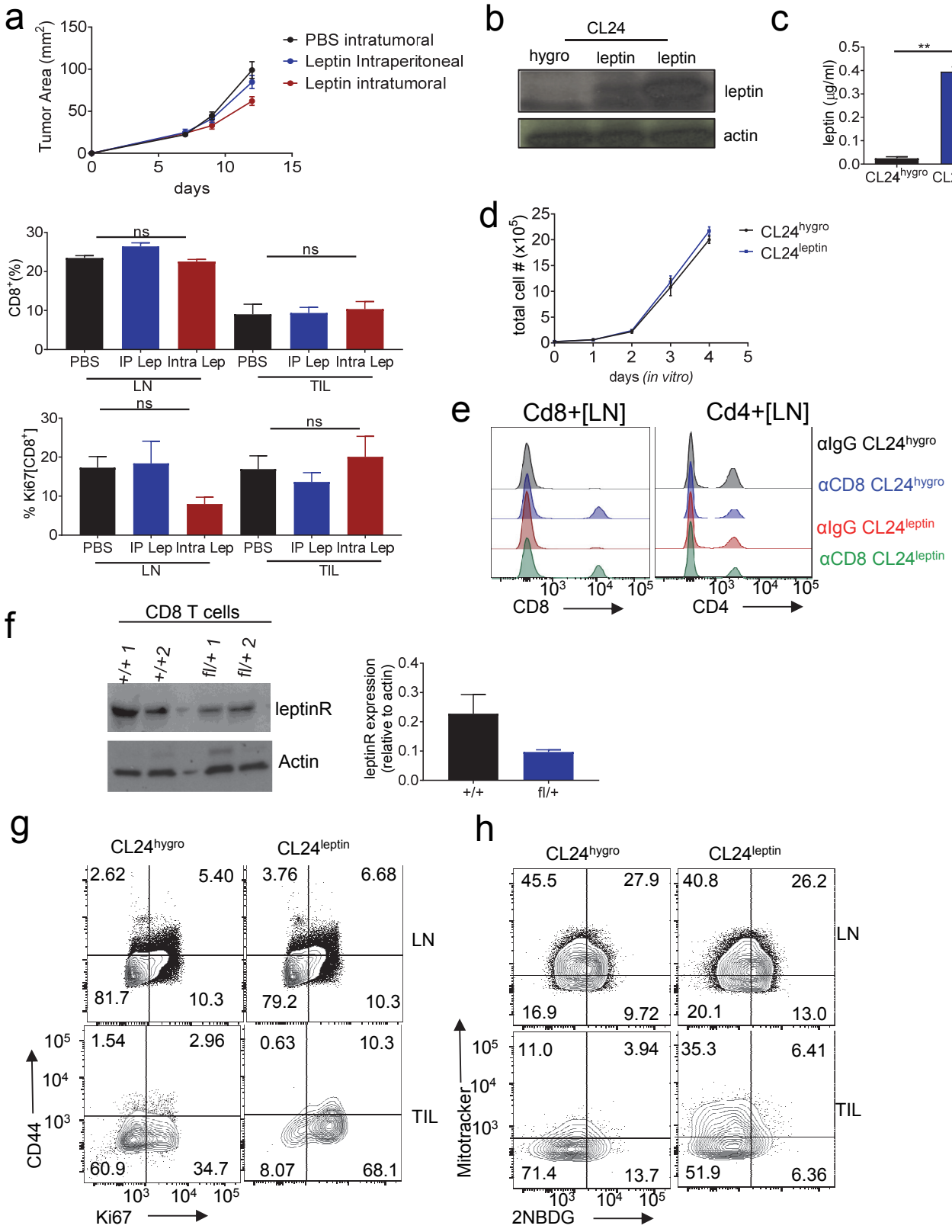
a
Tumor Area (mm2)
days
PBS intratumoral
Leptin Intraperitoneal
Leptin intratumoral
b
CL24
hygro
leptin
leptin
leptin
actin
c
leptin (µg/ml)
CL24hygro
CL24leptin
d
total cell # (x10^5)
days (in vitro)
CL24hygro
CL24leptin
CD8+(%)
% Ki67[CD8+]
PBS
IP Lep
Intra Lep
LN
TIL
ns
e
Cd8+[LN]
Cd4+[LN]
αIgG CL24hygro
αCD8 CL24hygro
αIgG CL24leptin
αCD8 CL24leptin
CD8
CD4
f
CD8 T cells
+/+ 1
+/+2
fl/+ 1
fl/+ 2
leptinR
Actin
leptinR expression (relative to actin)
+/+
fl/+
g
CL24hygro
CL24leptin
LN
TIL
CD44
Ki67
h
CL24hygro
CL24leptin
LN
TIL
Mitotracker
2NBDG

Figure S3

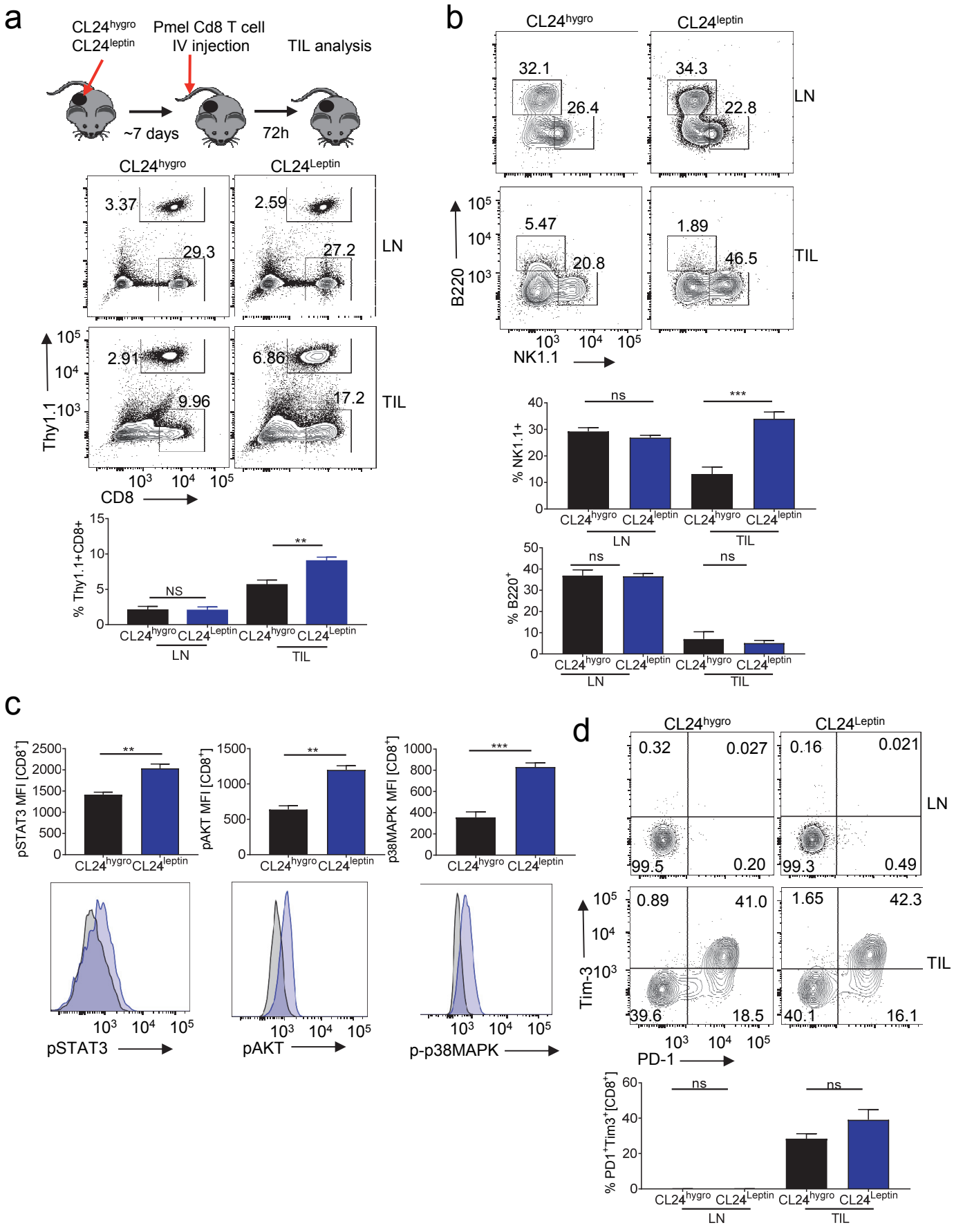
a
CL24hygro
CL24leptin
Pmel Cd8 T cell
IV injection
TIL analysis
~7 days
72h
CL24hygro
CL24Leptin
3.37
29.3
2.59
27.2
LN
Thy1.1
2.91
9.96
6.86
17.2
TIL
CD8
% Thy1.1+CD8+
NS
**
b
CL24hygro
CL24leptin
32.1
26.4
34.3
22.8
LN
B220
5.47
20.8
1.89
46.5
TIL
NK1.1
% NK1.1+
ns
***
% B220+
c
pSTAT3 MFI [CD8+]
pAKT MFI [CD8+]
p38MAPK MFI [CD8+]
pSTAT3
pAKT
p-p38MAPK
d
CL24hygro
CL24Leptin
0.32
0.027
0.16
0.021
LN
99.5
0.20
99.3
0.49
Tim-3
0.89
41.0
1.65
42.3
TIL
39.6
18.5
40.1
16.1
PD-1
% PD1+Tim3+[CD8+]

Figure S4

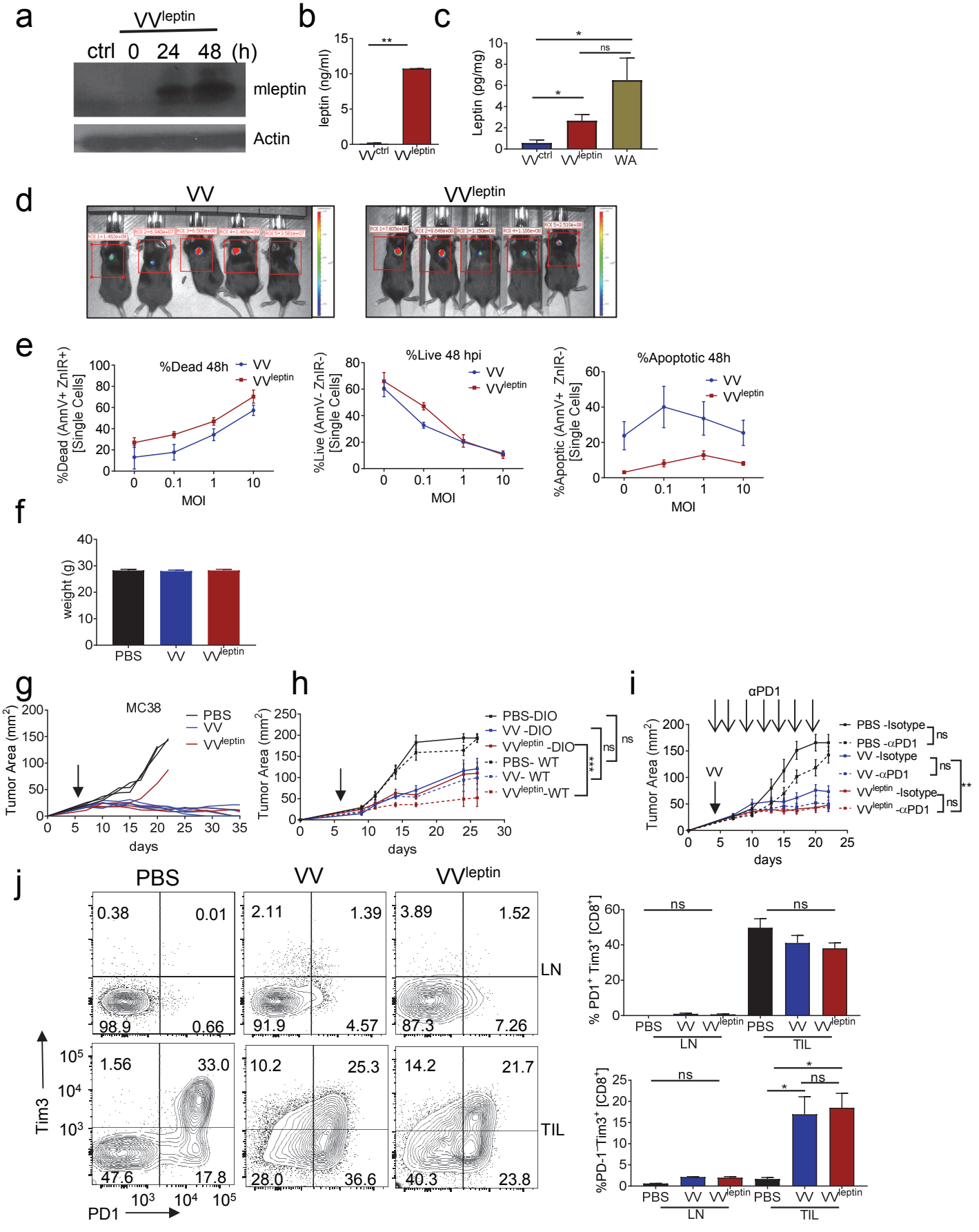
a
VVleptin
ctrl 0 24 48 (h)
mleptin
Actin
b
leptin (ng/ml)
VVctrl
VVleptin
c
Leptin (pg/mg)
VVctrl
VVleptin
WA
d
VV
VVleptin
e
%Dead 48h
VV
VVleptin
%Dead (AnnV+ ZnIR+) [Single Cells]
MOI
%Live 48 hpi
%Live (AnnV- ZnIR-) [Single Cells]
%Apoptotic 48h
%Apoptic (AnnV+ ZnIR-) [Single Cells]
f
weight (g)
PBS
VV
VVleptin
g
MC38
PBS
VV
VVleptin
Tumor Area (mm2)
days
h
PBS-DIO
VV -DIO
VVleptin -DIO
PBS- WT
VV- WT
VVleptin-WT
ns
***
i
αPD1
VV
PBS -Isotype
PBS -αPD1
VV -Isotype
VV -αPD1
VVleptin -Isotype
VVleptin -αPD1
ns
**
j
PBS
VV
VVleptin
0.38
0.01
98.9
0.66
2.11
1.39
91.9
4.57
3.89
1.52
87.3
7.26
LN
1.56
33.0
47.6
17.8
10.2
25.3
28.0
36.6
14.2
21.7
40.3
23.8
TIL
Tim3
PD1
% PD1+ Tim3+ [CD8+]
%PD-1+Tim3+ [CD8+]
LN
TIL

Figure S5

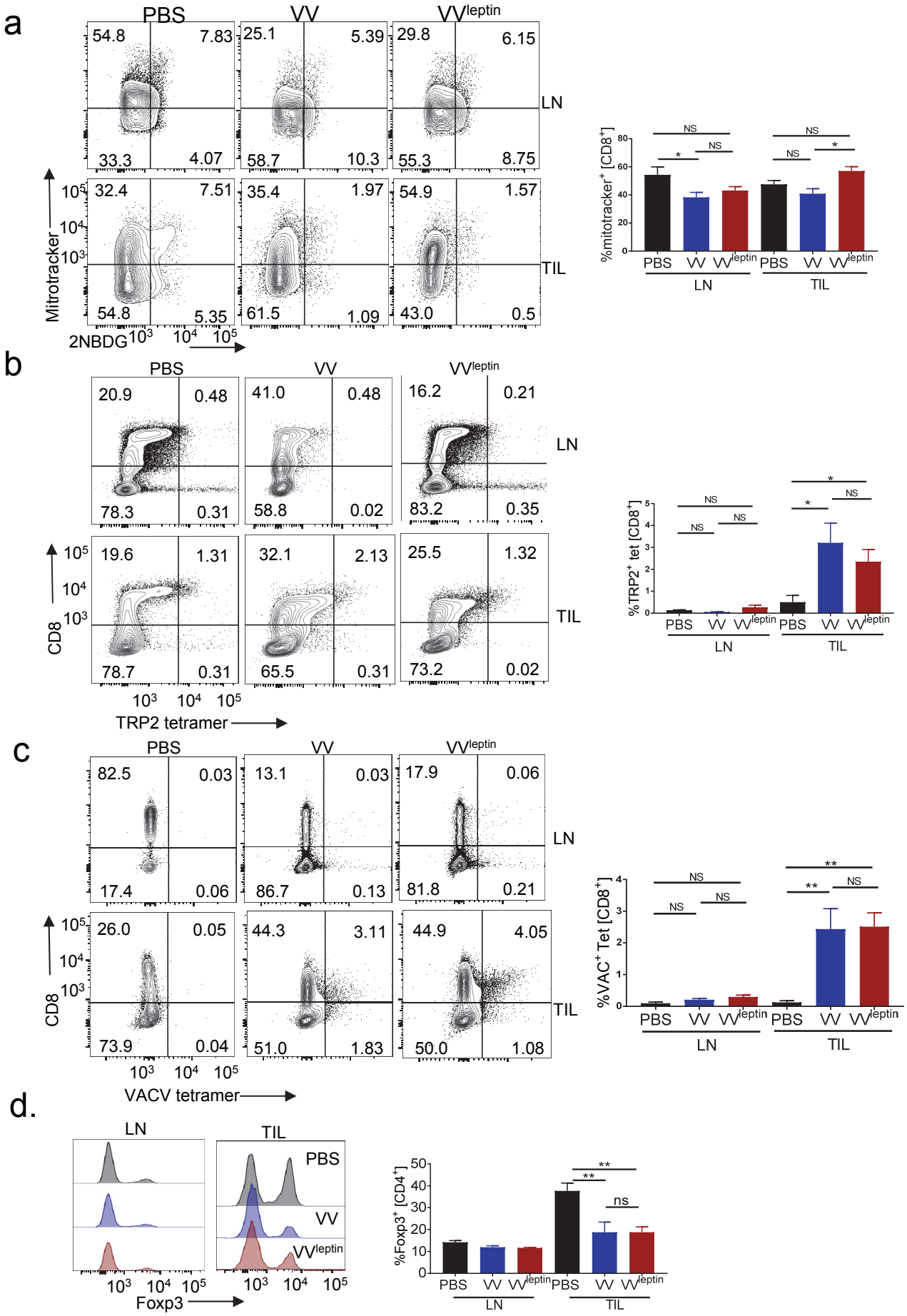
a
PBS
VV
VVleptin
54.8
7.83
25.1
5.39
29.8
6.15
LN
33.3
4.07
58.7
10.3
55.3
8.75
Mitrotracker
2NBDG
32.4
7.51
35.4
1.97
54.9
1.57
TIL
54.8
5.35
61.5
1.09
43.0
0.5
%mitotracker+ [CD8+]
NS
*
LN
TIL
b
20.9
0.48
41.0
0.48
16.2
0.21
78.3
0.31
58.8
0.02
83.2
0.35
CD8
19.6
1.31
32.1
2.13
25.5
1.32
78.7
0.31
65.5
0.31
73.2
0.02
TRP2 tetramer
%TRP2+ tet [CD8+]
c
82.5
0.03
13.1
0.03
17.9
0.06
17.4
0.06
86.7
0.13
81.8
0.21
26.0
0.05
44.3
3.11
44.9
4.05
73.9
0.04
51.0
1.83
50.0
1.08
VACV tetramer
%VAC+ Tet [CD8+]
**
d.
LN
TIL
PBS
VV
VVleptin
Foxp3
%Foxp3+ [CD4+]
ns

Figure S6

a

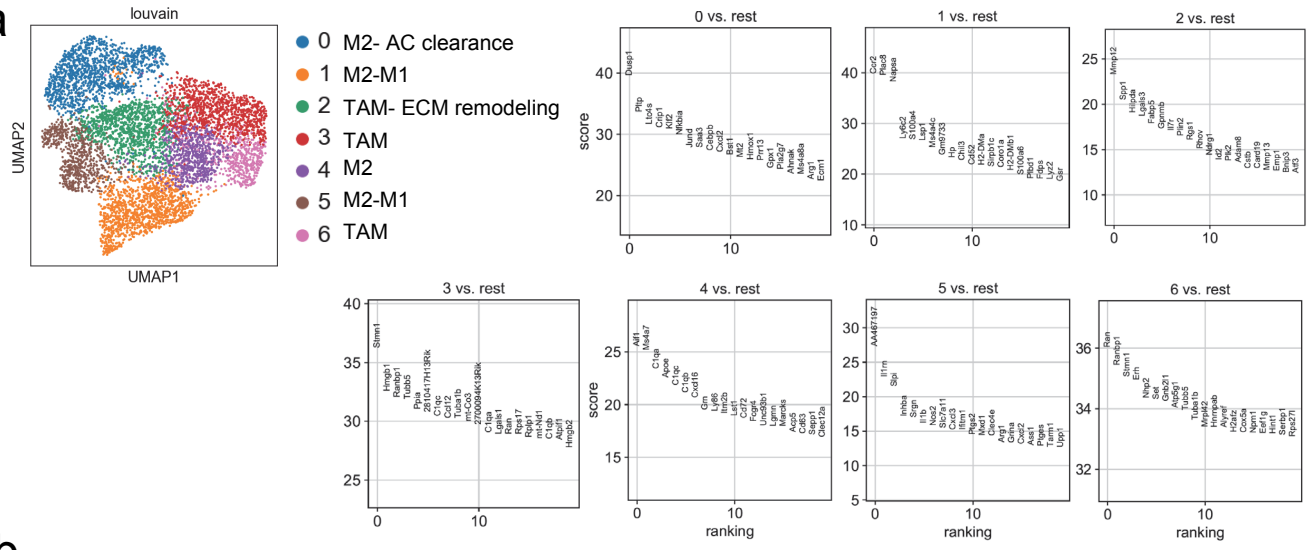
louvain
UMAP2
UMAP1
0 M2- AC clearance
1 M2-M1
2 TAM- ECM remodeling
3 TAM
4 M2
5 M2-M1
6 TAM
0 vs. rest
1 vs. rest
2 vs. rest
3 vs. rest
4 vs. rest
5 vs. rest
6 vs. rest
score
ranking

b

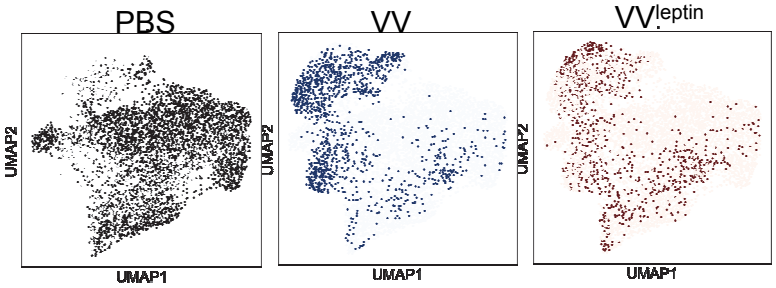
PBS
VV
VV.leptin
UMAP2
UMAP1

SUPPLEMENTARY FIGURE LEGENDS

Figure S1 related to Figure 1. Single cell RNA sequencing analysis from TIL treated with oncolytic *Vaccinia* virus. (A) Dot plot of top 5 differentially expressed genes defining each cluster of cells. Intensity of red color indicates the normalized level of gene expression and the size of the dot represents the percentage of cells expressing that gene. (B) UMAP plots with canonical marker genes colored which were used to assign identities to cell clusters. (C) Top 20 differentially expressed genes in each cluster as compared to all the other clusters.

Figure S2 related to Figure 4. Systemic delivery of recombinant leptin, characterization of leptin overexpression in tumor cells and leptin receptor knock out transgenics. (A) C57BL/6J mice were inject subdermally with CL24 cells. 5-7 days after injection tumors were treated either systemically by IP with recombinant leptin 3 consecutive or intratumorally (1ug/g) and tumor growth monitored. Representative flow histogram and tabulated flow cytometric data for CD8+ T cells from LN and TIL from mice and ki67 expression. (B) Immunoblot analysis of mouse leptin protein expression of CL24 cell line stably transduced with control plasmid ($CL24^{hygro}$) and mouse leptin gene plasmid ($CL24^{leptin}$). (C) ELISA analysis of leptin in the media of cells transduced with control plasmid and leptin gene. (D) In vitro growth analysis between $CL24^{hygro}$ and $CL24^{leptin}$ cell lines. (E) C57BL/6J mice were treated every other day with anti-CD8 (200ug). At day 6 mice were injected with either $CL24^{hygro}$ or $CL24^{leptin}$ and tumor growth was monitored. CD8 and CD4 expression analysis in lymph node (LN). (F) CD8 T cells isolated from ObR fl/+ CD4 CRE mice and analyzed by immunoblot for Leptin receptor (LeptinR), actin was used as a loading control. C57BL/6J mice were injected with either $CL24^{hygro}$ or $CL24^{leptin}$. (G) Representative flow cytogram of LN and TIL for metabolic markers MitoTracker FM staining and 2NBDG uptake. Error bars indicate s.e.m. Data represents at least 3 independent experiments *p <0.05, **p <0.01, ***p <0.001 by two-way ANOVA. Error bars indicate s.e.m.

Figure S3 related to Figure 4. Characterization of tumor infiltrating lymphocytes of leptin overexpression in tumor cells. (A) C57BL/6J mice were inject subdermally with $CL24^{hygro}$ and $CL24^{leptin}$ cells. 5-7 days after injection mice were given an adoptive transfer of $10x10^6$ previously activated PMEL CD8 T cells. 3 days after transfer tumors were analyzed for infiltrated

T cells. (B) NK1.1 and B220 analysis for natural killer cells and B cells respectively on LN and TIL from mice injected with $CL24^{hygro}$ and $CL24^{leptin}$. Representative flow histogram for NK1.1 and B220 staining in LN and TIL and tabulated flow cytometric data are shown. (C) Representative flow histogram and tabulated flow cytometric data for CD8+ T cells from LN and TIL from mice injected with $CL24^{hygro}$ and $CL24^{leptin}$ analyzed for pSTAT3, pAKT and p-p38MAPK expression. (D) Representative flow cytograms and tabulated flow cytometric data for Tim-3 and PD-1 expression leptin from tumors treated as in (B). Error bars indicate s.e.m. Data represents at least 3 independent experiments *p <0.05, **p <0.01, ***p <0.001 by two-way ANOVA. Error bars indicate s.e.m.

Figure S4 related to Figure 5. Additional tumor models and therapeutic regiments with leptin-engineered oncolytic *Vaccinia* virus and tumor infiltrating lymphocyte analysis
(A) Immunoblot analysis of mouse leptin protein expression of CL24 cell line treated with VV^{leptin} at $2.5x10^6$ PFU in vitro 24h and 48h. (B) ELISA analysis of leptin in the media of CL24 cells treated with VV^{leptin}. (C) ELISA analysis of leptin in interstitial fluid of tumors treated with VV or VV^{leptin}. Interstitial fluid from white adipose tissue (WA) used as control. Data represents at least 3 independent experiments *p <0.05 by two-way ANOVA. Error bars indicate s.e.m. (D) C57BL/6J mice were injected subdermally with CL24 cells. 5-7 days after tumor cell injection tumors were treated intratumorally with PBS, VV, or VV^{leptin} 24h later mice were injected with luciferin (30mg/ml) IP for 10min and conducted In Vivo Bioluminescence Imaging. (E) CL24 cells were infected in vitro with VV, or VV^{leptin} at MOI 01, 1, 10. Representative flow cytogram represents Zombie staining (live-dead) and AnnexinV (apoptosis). (F) C57BL/6J mice were injected subdermally with CL24 cells. 5-7 days after tumor cell injection tumors were treated intratumorally with PBS, VV, or VV^{leptin}. Mice were monitored for weight at the final time point of tumor growth analysis. (G) C57BL/6J mice were injected subdermally with MC38 cells. 5-7 days after tumor cell injection tumors were treated intratumorally with PBS, VV, or VV^{leptin}. Mice were monitored for tumor growth. (H) C57BL/6J DIO mice were injected subdermally with CL24 cells. 5-7 days after tumor cell injection tumors were treated intratumorally with PBS, VV, or VV^{leptin}. Mice were monitored for tumor growth. (I) C57BL/6J mice we treated as in (H) in addition to anti-PD1 treatment every other day. Mice were monitored for tumor growth. C57BL/6J mice were injected subdermally with CL24 cells. 5-7 days after tumor cell injection tumors were treated intratumorally with PBS, VV, or VV. Representative flow cytogram and tabulated flow cytometric data represents Tim-3 and PD1 expressions (J). Error bars indicate s.e.m. Data

represents at least 3 independent experiments *p <0.05, **p <0.01, ***p <0.001 by two-way ANOVA. Error bars indicate s.e.m.

Figure S5 related to Figure 5 and Figure 6. Tumor infiltrating lymphocyte analysis for after leptin-engineered oncolytic *Vaccinia* virus treatment. C57BL/6J mice were injected subdermally with CL24 cells. 5-7 days after tumor cell injection tumors were treated intratumorally with PBS, VV, or VV^{leptin}. Mice were monitored for tumor growth. (A) Representative flow cytogram and tabulated flow cytometric data represents mitotracker-2NBDG expression (A). C57BL/6J mice we treated as in (A) Representative flow cytogram and tabulated flow cytometric data represents CD8- TRP2 tetramer expression (B) and CD8 and Vaccinia tetramer expression (C). C57BL/6J mice we treated as in (A) Representative flow cytograms and tabulated flow cytometric data for $CD4^+$ $Foxp3^+$T cells (T regulatory cells) from LN and TIL (D). Error bars indicate s.e.m. Error bars indicate s.e.m. Data represents at least 3 independent experiments *p <0.05, **p <0.01, ***p <0.001 by two-way ANOVA. Error bars indicate s.e.m.

Figure S6 related to Figure 6. Single cell RNA sequencing analysis from TIL treated with oncolytic *Vaccinia* virus for macrophage subpopulation. (A) Unsupervised clustering of macrophage subpopulation. (B) Top 20 differentially expressed genes for each cluster seen in (A). (C) UMAPs colored by treatments depicting the cell distribution through the macrophage subpopulation clustering.